Available online at www.sciencedirect.com
SCIENCE DIRECT®
Tectonophysics 366 (2003) 113–141
TECTONOPHYSICS
www.elsevier.com/locate/tecto

Paleozoic northward drift of the North Tien Shan (Central Asia) as revealed by Ordovician and Carboniferous paleomagnetism

Mikhail L. Bazhenov[a,b], Adam Q. Collins[b], Kirill E. Degtyarev[a], Natalia M. Levashova[a], Alexander V. Mikolaichuk[c], Vladimir E. Pavlov[d], Rob Van der Voo[b,*]

[a] *Geological Institute, Academy of Sciences of Russia, Pyzhevsky Lane, 7, Moscow 109017, Russia*
[b] *Department of Geological Sciences, University of Michigan, 2534 C.C. Little Building, 425 E. University Ave., Ann Arbor, MI 48109-1063, USA*
[c] *Institute of Geology, National Academy of Sciences, 30 Erkindyk Av., Bishkek 720481, Kyrgyzstan*
[d] *Institute of Physics of the Earth, Academy of Sciences of Russia, Bolshaya Gruzinskaya St., 10, Moscow 123810, Russia*

Received 3 September 2002; accepted 28 February 2003

Abstract

Three new Middle–Late Ordovician and two new Early Carboniferous paleomagnetic poles have been obtained from the North Tien Shan Zone (NTZ) of the Ural–Mongol belt in Kyrgyzstan and Kazakhstan. Paleolatitudes for the Carboniferous are unambiguously northerly and average 15.5°N, whereas the Ordovician paleolatitudes (6°, 9°, and 9°) are inferred to be southerly, given that a very large (~ 180°) rotation of the NTZ would be necessary during the middle Paleozoic if the other polarity option was chosen. Thus, the NTZ drifted northward during much of the Paleozoic; east–west drift cannot be determined, as is well known, from paleomagnetic data. In addition, detailed thermal demagnetization analysis reveals two overprints, one of recent age and the other of Permian age, which is a time of strong deformation in the NTZ. The paleolatitude of the combined Permian overprint is 30.5 + 2°N. The paleolatitudes collectively track those predicted for the area by extrapolation from Baltica very well, but are different from those of Siberia for Ordovician times. This finding is compatible with Sengör and Natal'in's [Sengör, A.M.C., Natal'in, B.A., 1996. Paleotectonics of Asia: fragments of a synthesis. In: Yin A., Harrison, M. (Eds.), The Tectonic Evolution of Asia. Cambridge Univ. Press, Cambridge, pp. 486–640] model of tectonic evolution of the Ural–Mongol belt and disagrees with the models of other researchers. Declinations of the Ordovician and Early Carboniferous results range from northwesterly to northeasterly, and are clearly affected by local relative rotations, which seem characteristic for the entire NTZ, because the Permian overprint declinations also show such a spread. Apparently, the important latest Paleozoic–Triassic deformation involved shear zone-related rotations as well as folding and significant granitic intrusions.

Keywords: Tien Shan; Ordovician; Carboniferous; Paleolatitudes; Ural–Mongol fold belt; Paleopoles

1. Introduction

Eurasia comprises several Precambrian cratons divided by mobile zones of different ages. As such,

* Corresponding author. Tel.: +1-734-764-8322; fax: +1-734-763-4690.
E-mail address: voo@umich.edu (R. Van der Voo).

0040-1951/03/$ - see front matter © 2003 Elsevier Science B.V. All rights reserved.
doi:10.1016/S0040-1951(03)00075-1

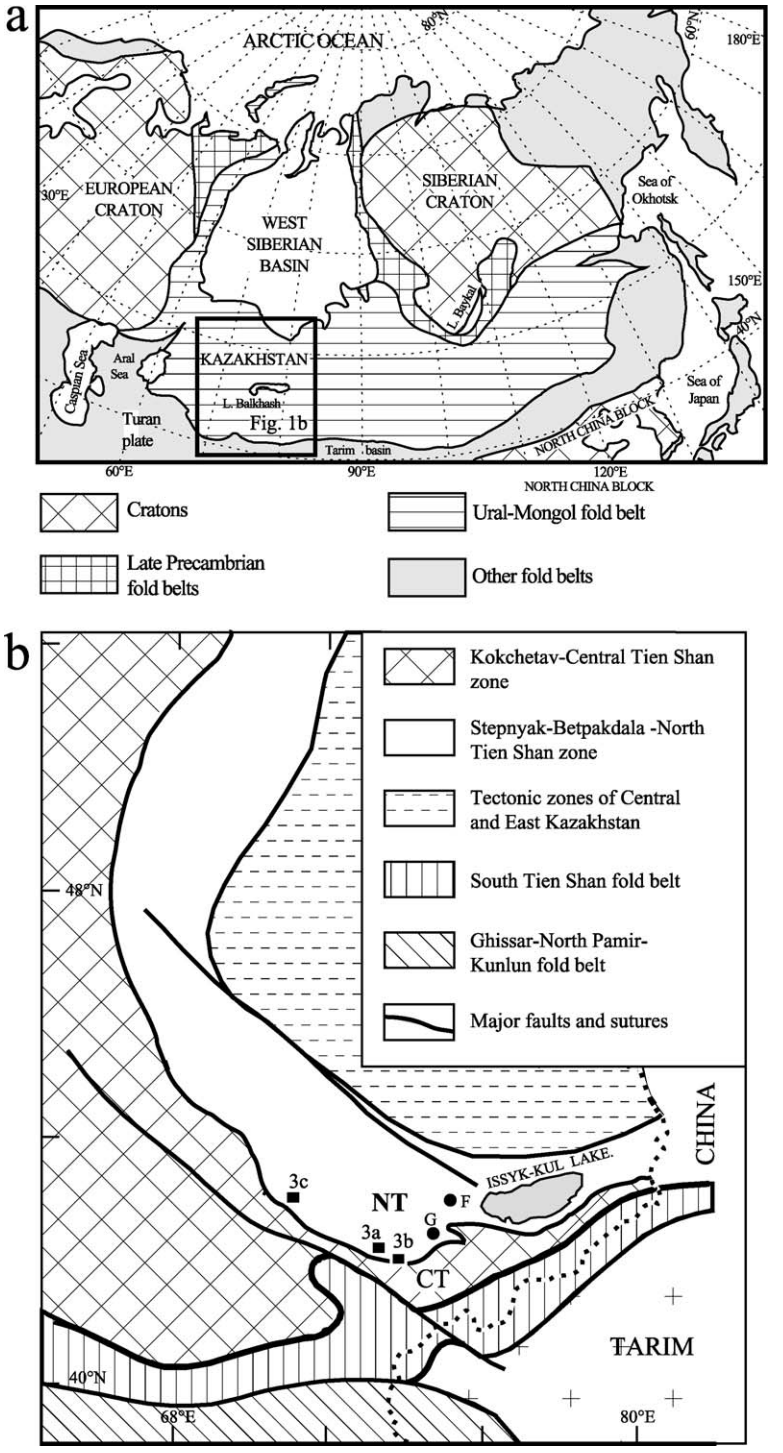
a
ARCTIC OCEAN
80°N
60°N
180°E
30°E
EUROPEAN CRATON
WEST SIBERIAN BASIN
SIBERIAN CRATON
Sea of Okhotsk
150°E
40°N
L. Baikal
KAZAKHSTAN
Aral Sea
Caspian Sea
L. Balkhash
Fig. 1b
Turan plate
Tarim basin
Sea of Japan
NORTH CHINA BLOCK
60°E
90°E
120°E
Cratons
Ural-Mongol fold belt
Late Precambrian fold belts
Other fold belts
b
Kokchetav-Central Tien Shan zone
Stepnyak-Betpakdala -North Tien Shan zone
Tectonic zones of Central and East Kazakhstan
South Tien Shan fold belt
Ghissar-North Pamir-Kunlun fold belt
Major faults and sutures
48°N
CHINA
ISSYK-KUL LAKE
3c
NT
F
G
3a
3b
CT
TARIM
40°N
68°E
80°E

it is a present-day counterpart of ancient supercontinents like Pangea, and Eurasian tectonics is the key to understanding their formation. One way to progress in this direction is to study the kinematics of the cratons. Even a cursory glance on a map, however, shows that the cratons occupy only about half of Eurasia, and the other half consists of the mobile belts (Fig. 1a). Thus another approach to understand the supercontinent formation is through tectonic evolution of these belts.

The largest mobile zones of Eurasia are the Alpine and Ural–Mongol fold belts. While the former is the locus of Eurasian growth in the Mesozoic to Cenozoic, the latter played the same role throughout the late Paleozoic. The Ural–Mongol fold belt crosses Eurasia from the North Urals to Kazakhstan and Tien Shan to Altai and Mongolia and on to the Pacific (Fig. 1a) and comprises many microcontinents with Precambrian crust and numerous subduction-related complexes separated by ophiolitic sutures (e.g. Mossakovsky et al., 1993; Didenko et al., 1994; Dobretsov et al., 1995). Most units are thought to have welded together by the Devonian, with post-collisional deformation of, and motions within, the Ural–Mongol belt being relatively small (e.g. Mossakovsky et al., 1993). A principally different view was expressed by Sengör et al. (1993) and Sengör and Natal'in (1996), who hypothesized that a huge continuous island arc (Kipchak Arc) was attached to the European and Siberian cratons beginning in the Vendian and was rifted away by the Cambrian. This arc was being deformed into a more complicated, but still continuous structure in the Cambrian through the Silurian. Since the Ordovician and especially since the Devonian, this structure was disrupted by large-scale strike-slips into separate segments, which were juxtaposed and amalgamated into a single block. Thus the original distribution of landmasses and the leading tectonic processes in the above models are very different. Geological and biostratigraphic data do not discriminate between the models; the latter show that the spatial distribution of some taxons better match one type of models, while other taxons favor the other (Burtman, 1999; S.G. Samygin, 2000, personal communication).

These models predict different kinematics of major tectonic units of the Ural–Mongol belt and can be tested with paleomagnetic data, especially on early and middle Paleozoic rocks. Available data, however, are scarce and often of poor quality; many key units have no data altogether. The importance of paleomagnetic data from the Ural–Mongol belt has long become clear to many, and several studies have already been undertaken. Unfortunately, most attempts failed because this region is strongly affected by a widespread late Paleozoic remagnetization (Pechersky and Didenko, 1995; Grishin et al., 1997; A.Y. Kazansky, personal communication). The situation is difficult but not hopeless as recent studies based on detailed cleaning and principal component analysis succeeded in isolation of primary components from middle to late Paleozoic rocks from northeastern Kazakhstan (Didenko and Morozov, 1999).

The North Tien Shan tectonic zone, NTZ, and its counterparts in Kazakhstan (Fig. 1b) are major units in the central part of the Ural–Mongol belt, and the NTZ kinematics is crucial in discriminating between the competing tectonic models. Paleozoic paleomagnetic data on the NTZ are very scarce; we present new Ordovician and Carboniferous results from the NTZ in this article and discuss their tectonic implications.

2. Geological setting and sampling

The NTZ sensu stricto trends E–W parallel to the modern mountains for about 500 km in North Kyrgyzstan and South Kazakhstan; the eastward continuation of this zone into the Chinese Tien Shan is ambiguous (Mazarovich et al., 1995). In the west, the zone can be traced into the Stepnyak–Betpakdala zone in Kazakhstan (Fig. 1b). Despite lateral variation in structure and sections, the Stepnyak–Betpakdala zone and the NTZ have been regarded by some

Fig. 1. (a) Location map of the Ural–Mongol fold belt. (b) Main early Paleozoic tectonic units of Kazakhstan (simplified after (Avdeev and Kovalev, 1989; Yakubchuk, 1990; Zamaletdinov and Osmonbetov, 1988)). NT, North Tien Shan; CT, Central Tien Shan. Solid squares: Toluk, Tabylgaty, and West Kyrgyz Range sampling localities shown in Fig. 3a–c, respectively. Solid circles labeled F and G: sampling localities of Permian rocks from Bazhenov et al. (1999).

geologists as a single first-order tectonic unit about 2000 km in length (Nikitin, 1972, 1973).

In the NTZ, shelf and continental slope complexes of Precambrian age outcrop as disrupted blocks and thrusts, and their original relationship is unclear. Cambrian to Lower Arenigian rocks include subduction-related volcanics, marginal sea, rift, and passive margin complexes, which are regarded as the remnants of a basin with oceanic crust—the Terskey Ocean or marginal sea (Mikolaichuk et al., 1997; Degtyarev and Mikolaichuk, 1998). The closure of this basin by the Early–Middle Arenigian boundary resulted in thrusting and deformation of all older complexes and some granite intrusions.

Middle Arenigian conglomerate and olistostromes overlap the Cambrian–Early Arenigian complexes with a major angular unconformity (Fig. 2). A thick pile of differentiated volcanics of Late Arenigian to Early Caradocian age accumulated in the northern and central parts of the NTZ; this series is considered an equivalent of modern active continental margins (Lomize et al., 1997). Along the southern boundary of the NTZ, volcanics are replaced by terrigenous and volcanoclastic rocks of the same age, which are locally intruded by relatively small bodies of acid to intermediate magmatic rocks (II in Fig. 2) and covered with erosional disconformity by Upper Ordovician red sandstones with siltstone and limestone interbeds. The sequence is intruded by numerous large granite bodies during the Late Ordovician (III in Fig. 2), and smaller granites were emplaced in the Silurian (Mikolaichuk et al., 1997). Due to the lack of Silurian rocks in most of the NTZ, the age of deformation here cannot be constrained better than pre-Early Devonian. A major angular unconformity, however, is present at the Ordovician–Silurian boundary in the Stepnyak–Betpakdala zone of Kazakhstan (Nikitin, 1972, 1973), and it is likely that the NTZ was strongly deformed at about this time as well. On a broader scale, geological data indicate that the Stepnyak–Betpakdala zone and the NTZ were welded to other major blocks of Kazakhstan during the Silurian (Mossakovsky et al., 1993).

Lower–Middle Devonian basic and acid subaerial volcanics in the North Tien Shan reside with a major unconformity on lower Paleozoic rocks (Fig. 2). In Late Devonian–Middle Carboniferous time, a carbonate platform existed to the south in the Central (Median) Tien Shan (Fig. 1b); the carbonate platform complex is laterally traced over 1000 km (Alexeiev et al., 2000). A deep basin filled with terrigenous rocks appeared between the carbonate platform and the NTZ in the late Tournaisian. The northern part of the basin which onlaps the NTZ is filled with Upper Visean to Lower Bashkirian redbeds (Mikolaichuk et al., 1995).

The carbonate platform complex was thrust over the NTZ in Middle Bashkirian time. The thrusts are sealed by Upper Carboniferous conglomerates with subordinate sandstone and siltstone, which are in turn overlain with erosional unconformity and basal conglomerate by Permian volcanics (Fig. 2). A prominent angular unconformity between the Permian and Lower Jurassic rocks indicates strong deformation in the latemost Paleozoic and/or Triassic. Finally, the entire Tien Shan was affected by alpine tectonism. It should be stressed that the intensities of deformation events are laterally variable, and it is often difficult to evaluate the magnitudes of each deformation at a locality.

Our studies concentrated on three areas close to the southern margin of the NTZ (Figs. 1b and 3). The Toluk area (Fig. 3a) is occupied by a NW–SE trending syncline formed by gray terrigenous and volcanoclastic rocks of Middle Arenigian to Early Caradocian age (Zima and Maksumova, 1990; Misius, 1993; Mikolaichuk et al., 1997). Gray rocks are conformably overlain by red sandstones with siltstone and limestone interbeds which outcrop in the fold core. Brachiopods from the basal redbeds correspond to the *Climacograptus wilsoni* graptolite zone and point to a Middle Caradocian age (Misius, 1993); the entire redbed suite can be considered Late Caradocian in age (Misius, 1993). Lower Paleozoic rocks are overlain with angular unconformity by Lower Carboniferous redbeds, which are in turn covered by weakly deformed upper Cenozoic sediments.

Gray sandstones and siltstones of Late Arenigian–Llanvirnian to Early Caradocian ages were sampled from the northeastern limb of a large syncline (sites ToG1 to ToG4) and in the northern part of the Toluk area, where the dips are generally to the north (sites ToG5 to ToG7). Upper Caradocian redbeds were taken from both limbs of the same syncline (sites ToR1 to ToR7). In total, 81 samples of gray rocks and 93 samples of redbeds were taken.

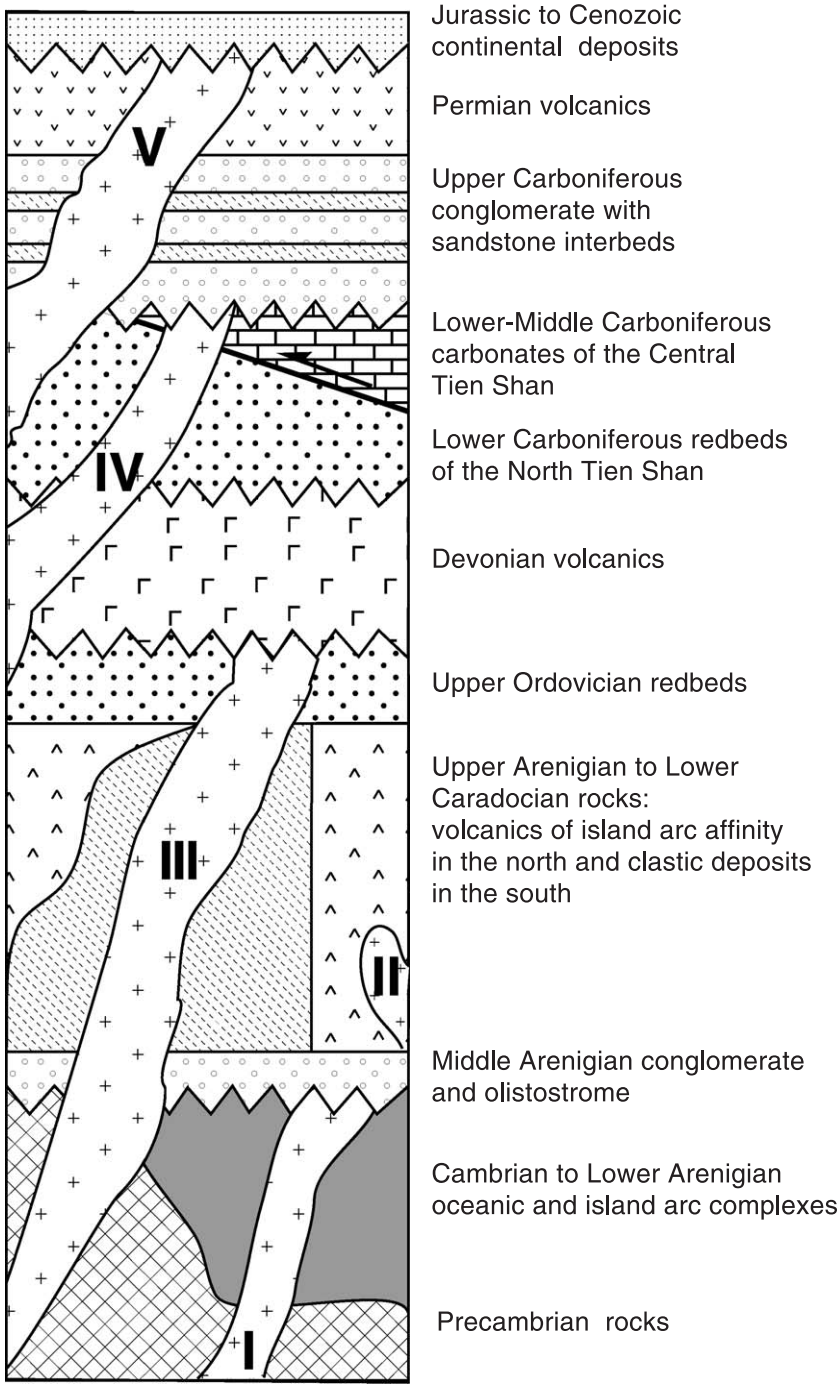

Fig. 2. Generalized geological column of the North Tien Shan. Saw-toothed lines, angular unconformities; thick solid line, thrust between terrigenous rocks of the North Tien Shan in the north and carbonates of the Central Tien Shan in the south. Cross-filling, granite intrusions of various age: I, Early Ordovician; II, Middle Ordovician; III, Late Ordovician and Early Silurian; IV, Middle Carboniferous; V, Permian. Note that this column is schematic, and there are minor lateral facies changes.

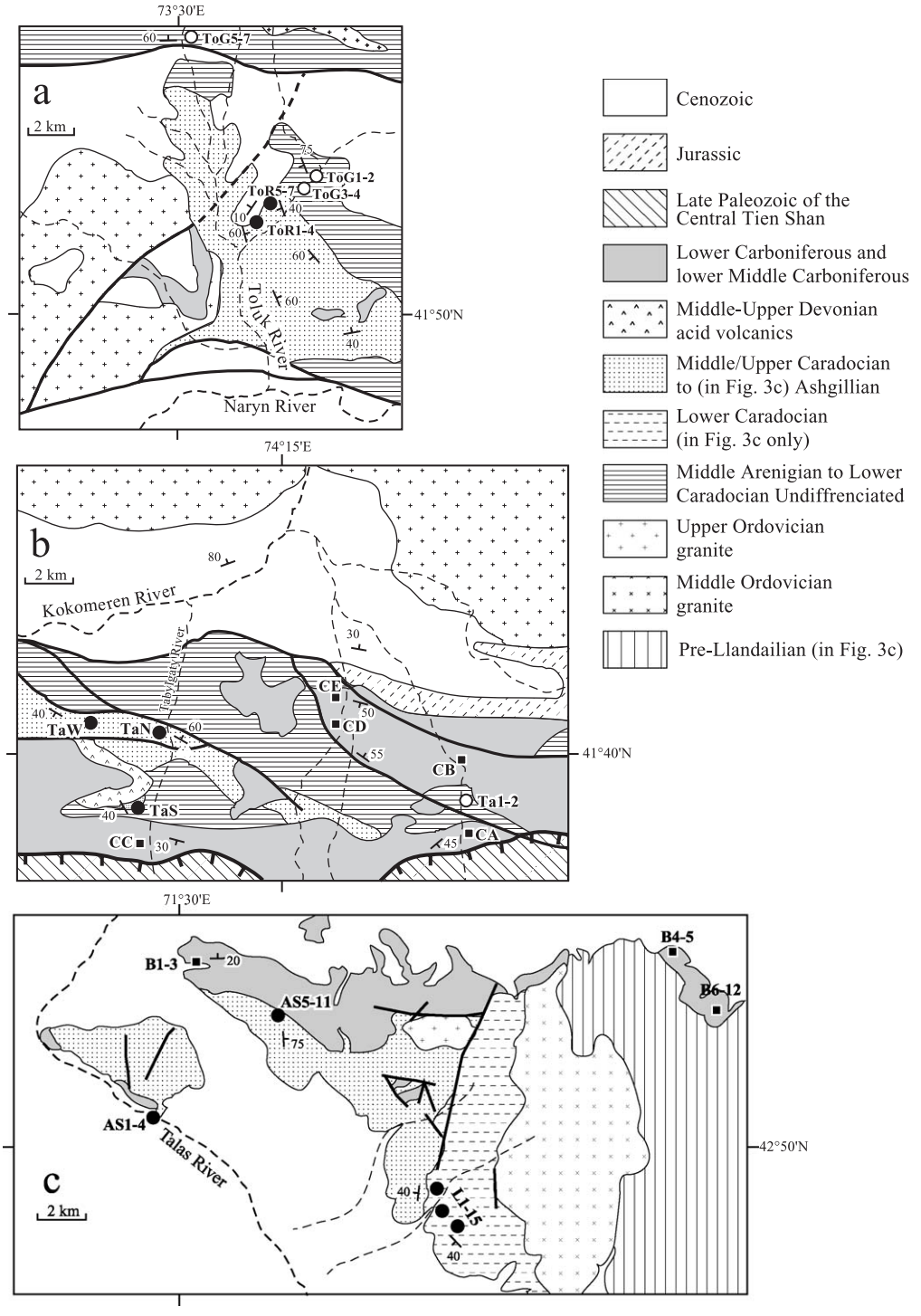

Fig. 3. Schematic geological maps of the Toluk (a), Tabylgaty (b), and West Kyrgyz Range (c) areas. Toothed line is the major thrust between the Central and North Tien Shan. Solid (dashed) lines are mapped (inferred) faults. Sampling localities of Middle Ordovician, Upper Ordovician, and Lower Carboniferous rocks labeled as in the text are shown by open circles, solid circles, and solid squares, respectively.

In the Tabylgaty area (Fig. 3b), the oldest rocks are Middle Ordovician gray terrigenous sediments almost without volcanoclastic input, which are conformably overlain by red sandstones with siltstone and limestone interbeds. Inarticulate brachiopods from redbeds indicate that these rocks accumulated during the later part of the *C. wilsoni* and the earlier part of the *Dicranograptus clingani* graptolite zones (Misius, 1986). Thus the Tabylgaty redbeds are also of Late Caradocian age.

Twelve samples of Middle Ordovician gray sandstones and siltstones were collected from two sites Ta1 and Ta2. In contrast to the Toluk area, Upper Caradocian redbeds here do not outcrop as a continuous structure, and 128 samples were taken from three isolated monoclinal sections (localities TaS, TaN, and TaW; Fig. 3b).

In the same (Tabylgaty) area, more than 1000-m-thick Lower Carboniferous rocks (the Dungurma Fm.) reside with angular unconformity on the Ordovician sequence and Middle–Upper Devonian age acid volcanics. The basal member of the Dungurma Fm. includes interbedded gray and red to brown-red conglomerates, gritstones, sandstones, and siltstones with limestone intercalations. Numerous foraminifera (V.P. Skvortsov, unpublished data) and brachiopods (A.L. Galitskaya, unpublished data) point to a Late Visean–Early Serpukhovian age of the basal member. Brachiopods, corals, and foraminifera (Galitskaya and Korolev, 1961) indicate a Serpukhovian age of the middle and upper parts of the Dungurma Fm. The Dungurma beds are overthrust from the south by the carbonate platform complex of the Central Tien Shan in the Middle Bashkirian (Figs. 2 and 3b).

The Dungurma Fm. was sampled at five localities, CA to CE (Fig. 3b). Rose-gray, brick-red, and gray sandstones were sampled at localities CA and CC from the lower part of the formation close to the thrust separating terrigenous redbeds of the North Tien Shan and late Paleozoic carbonates of the Central Tien Shan. Brown-red sandstones and siltstones were sampled at localities CB, CD, and CE from the upper member of this formation. In total, 143 hand samples were taken at 20 sites from beds of various attitudes.

At the western termination of the Kyrgyz Range (Fig. 3c), Precambrian to Middle Ordovician rocks are intruded by a granite body of Middle Ordovician age (464.1 ± 1 Ma on zircons (Kiselev, 1999)) that is overlain with erosional unconformity and basal conglomerate by several-hundred-meter-thick red sandstones of the Almaly Fm. of Caradocian, most likely Early Caradocian age. The Almaly Fm. is conformably covered by a 1500-m-thick pile of coarse- to medium-grained green sandstones (Tasbeksy Fm.) with transitional Caradocian–Ashgillian inarticulate brachiopods in the upper half of this pile (I.F. Nikitin, personal communitation). Several hundred meters upsection, the green rocks are conformably covered by a 200- to 300-m-thick red siltstones and fine-grained sandstones (Botmoynak Fm.) of most likely Ashgillian age. Ordovician rocks are intruded in the central part of the map area by a granite body and minor dikes of intermediate composition of presumed latemost Ordovician to Early Silurian age. With major angular unconformity and basal conglomerate, Visean–Serpukhovian strata reside on all older rocks. They are conformably and with a gradual transition replaced by Bashkirian (lower Middle Carboniferous) continental redbeds with visible thickness of up to 150 m, which were deformed both in the late Paleozoic and late Cenozoic.

Lower Caradocian redbeds of the Almaly Fm. were sampled from 15 sites (120 samples in total) in the southern part of the area from beds with moderate dips and azimuths varying from WNW to almost due south. Ashgillian redbeds of the Botmoynak Fm. were sampled from two separate localities (Fig. 3c). Sites AS1 to AS4 (24 samples) are from an about 30-m-thick exposure on both banks of the Talas River where these rocks are gently dipping to the WSW and show no signs of penetrative deformation. A thicker section of this formation was found to the north; these rocks, however, are cleavaged. From six sites, AS5 to AS11, 63 samples were taken from the visibly least deformed parts of this section. The beds here dip steeply to the east; graded bedding in several beds indicates normal position of this section. Also sampled were 20 fragments of these redbeds from the overlying Lower Carboniferous basal conglomerate.

Carboniferous redbeds are gently dipping to the north in the western part of the area (sites B1 to B3). Deformation is more both intense and variable in the east where samples were taken from the beds in overturned position (sites B4 to B5) and from both

limbs of a small syncline (sites B6 to B12); in total, 95 samples were taken.

3. Methods

The true thickness studied at each site varies from several meters to several tens of meters, and samples were distributed more or less uniformly across the outcrops. Well-stratified rocks were studied everywhere, and bedding measurements are available for most samples; hence at most sites, we used these data for tectonic correction instead of site-averaged values. This may account for the changes in statistical parameters upon tilt correction. Oriented samples were collected either as hand-blocks or with a gasoline-powered drill and oriented with a magnetic compass. One cubic specimen from each hand block was subjected to progressive thermal demagnetization in 15–20 steps up to 690 °C in a homemade oven with internal residual fields of ~ 10 nT and measured with a JR-4 spinner magnetometer having a noise level of 0.05 mA/m in the Paleomagnetic Laboratory of the Geological Institute in Moscow. Many samples of Ordovician redbeds were found to have acquired spurious remanence above 600 °C thus preventing further cleaning. As a result, some duplicate Ordovician specimens from the Toluk area were thermally demagnetized in a multishield furnace and measured with a cryogenic magnetometer in a nonmagnetic room in the Paleomagnetic Laboratory of the Institut de Physique du Globe in Paris. Still other duplicate Ordovician samples from the Tabylgaty area and most samples of Ordovician and Carboniferous rocks from the West Kyrgyz Range were thermally demagnetized with an Analytical Services shielded oven and measured with a 2-G cryogenic magnetometer in a nonmagnetic room in the Paleomagnetic Laboratory of the University of Michigan in Ann Arbor. Demagnetization quality proved to be very similar in all the laboratories and is not differentiated further on. Demagnetization results were plotted on orthogonal vector diagrams (Zijderveld, 1967), and component directions and remagnetization circles were identified with the aid of principal component analysis (Kirschvink, 1980). The characteristic remanent magnetization (ChRM) was determined with anchoring the final linear segments to the origin of the vector diagrams. Components isolated from sister specimens of a hand sample were used to calculate the sample means, which were in turn used to calculate site means. If two specimens yielded only remagnetization circles, a longer and more precise circle was chosen for combining direct observations and remagnetization circles (McFadden and McElhinny, 1988).

4. Results

4.1. Ordovician rocks

4.1.1. Toluk area

Upper Arenigian–Upper Caradocian rocks showed very variable demagnetization characteristics (Fig. 4). Some samples showed nearly no change in both direction and magnitude from 200 to 500 °C and a rectilinear decay to the origin afterwards (component C, Fig. 4a), while adjacent samples may be heavily overprinted by a remanence (component A) whose direction in situ is close to the present-day field (Fig. 4b). These two components can strongly overlap (Fig. 4c), or component A only can be isolated (Fig. 4d). In still other samples, a component (B) with moderately steep upward inclination and southward declination in situ is present, either as the only component (Fig. 4e) or preceded by component A (Fig. 4f). If component B is present in a sample, treatment above 600 °C was prevented by acquisition of strong spurious remanence, most likely because of mineralogical alteration. As a result, component C could not be isolated from such samples, and remagnetization circles using steps at intermediate to high temperatures were utilized for analysis. Mineralogical alteration close to 600 °C took place in some samples, which behaved at lower temperatures (Fig. 4g) similarly to those where only component C is found (Fig. 4a); in such cases, Fisher means of the corresponding clusters were used.

Component A is of normal polarity everywhere and best clusters in situ. Its overall mean insignificantly differs from the present-day field direction. Hence this remanence was acquired after late Cenozoic minor tilting in the area.

The second component (B) is isolated at intermediate temperatures from four or more samples at each of four redbed sites (ToR, Table 1). The corre-

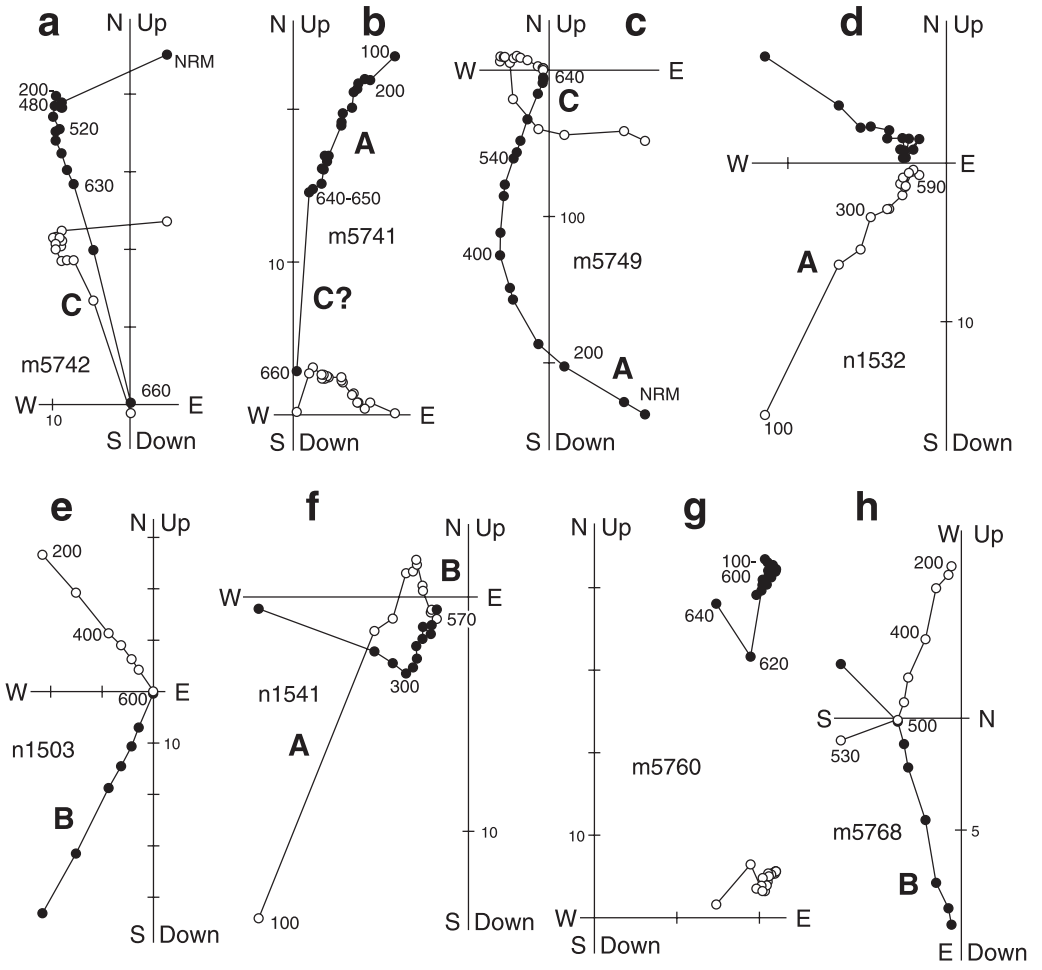

Fig. 4. Representative thermal demagnetization plots of Ordovician rocks from the Toluk area in stratigraphic coordinates. Capital characters close to the plots denote paleomagnetic components (see text). Full (open) dots represent vector endpoints projected onto the horizontal (vertical) plane. Temperature steps are in °C. Magnetization intensities are in mA/m. Thick dashed lines denote isolated components labeled as in the text (shown only on some plots). For clarity, NRM points are omitted from most plots.

sponding linear segments usually miss the origin; hence this remanence is likely to be an overprint. Upon tilt correction, the scatter of component B directions increases drastically (Table 1, squares in Fig. 5a,b).

Component C has the highest unblocking temperatures and shows rectilinear decay to the origin where it can be reliably isolated. It is destroyed above 650 °C implying hematite as the carrier. Component C has two polarities at each limb. After tilt correction, the site means have similar inclinations but divergent declinations (Table 2; Fig. 5f,g). The inclination-only fold test (McFadden and Reid, 1982) is positive, and the minimal dispersion of inclinations is observed at 100% unfolding. Thus component C is prefolding and therefore definitely pre-Early Devonian and likely pre-Early Silurian, as discussed above.

Gray rocks at sites ToG5–7 revealed no consistent pattern during demagnetization. At sites ToG1–4, linear segments clearly miss the origin (Fig. 4h) and define a component with in situ directions, which resemble those of component B in the redbeds (Table 1). The component B data from the both rock

Table 1
Mean directions of component b in Upper Arenigian–Upper Caradocian rocks from the North Tien Shan

S/L	*N*	B	In situ				Tilt-corrected			
			D (°)	*I* (°)	*k*	α_{95} (°)	*D* (°)	*I* (°)	*k*	α_{95} (°)
Toluk area										
ToR1	16/8	65/38	205.1	−38.1	38	9.2	214.4	−6.1	38	9.2
ToR3	9/7	68/42	219.3	−44.5	26	11.9	227.8	−5.4	24	12.4
ToR4	9/4	69/60	202.9	−36.9	38	15.2	213.2	10.3	38	15.2
ToR5	14/9	249/47	197.2	−29.6	6	24.0	159.5	−46.9	6	22.6
R	(4)		205.6	−37.5	72	10.9	208.4	−12.6	5	43.8
ToG1	10/6	240/72	209.7	−65.9	17	16.9	74.6	−38.3	20	15.2
ToG2	10/3	252/68	186.4	−41.5	86	13.3	125.6	−32.1	26	24.8
ToG3	9/5	259/76	222.3	−57.2	31	14.0	103.5	−38.7	31	14.0
G	(3)		203.4	−55.9	24	25.7	102.0	−38.2	15	32.7
G+R	(7)		204.8	−45.3	28	11.5	169.9	−36.0	<3	53.7
Tabylgaty area										
TaN1	11/9	29/66	304.0	−21.6	8	19.4	276.8	−22.6	8	19.4
TaN2	10/8	16/59	311.5	−12.2	22	11.9	285.0	−35.5	24	11.6
TaN3	12/10	4/65	296.5	−23.8	14	13.6	254.5	−35.2	23	10.4
TaN4	10/8	327/60	297.9	−37.5	18	13.2	240.6	−50.5	14	15.2
TaN	(4)		302.8	−23.9	44	14.0	266.1	−37.1	18	22.5
TaS3+4	17/7	225/38	247.4	−68.8	28	11.6	21.7	−70.1	20	13.7
TaW2	11/6	202/39	262.3	−47.8	11	21.0	312.2	−51.3	11	20.7
S+W	13		251.4	−59.5	13	11.7	333.8	−65.8	9	14.6

S/L, sites/localities labeled as in the text and Fig. 3; G, R, and G+R, gray rocks, redbeds, and all rock types, respectively; *N*, number of samples (sites in parenthesis) studied/accepted; *B*, azimuth of dip/dip angle; *D*, declination; *I*, inclination; *k*, concentration parameter (Fisher, 1953); α_{95}, radius of 95% confidence circle.

types are combined, and site means are best grouped in situ (Fig. 5a,b); hence this component is postfolding and post-Early Silurian. No high-temperature component could be isolated from the gray rocks (ToG sites).

4.1.2. Tabylgaty area

Gray rocks from sites Ta1–2 revealed no consistent pattern during demagnetization. In the redbeds, demagnetization characteristics and paleomagnetic results vary from locality to locality. Similar to the Toluk area, components A, B, and C can be recognized in the Tabylgaty area (Fig. 6).

Many samples from locality TaS showed rectilinear decay to the origin (component C) after the removal of a weak overprint (component A) above 300 to 400 °C (Fig. 6a,b). Some samples give noisier data, but the same components can be recognized too (Fig. 6c). And in just a few samples, a weak component B can be recognized at intermediate temperatures (Fig. 6d).

Redbeds from locality TaW generally yield noisier data, the rectilinear decay to the origin being observed in a few samples (Fig. 6e). In some samples, the overprint has negative inclination and southwesterly declination in situ (component B) (Fig. 6f), while the overprint is close to the present-day field

Fig. 5. Stereoplots of component directions in Upper Ordovician redbeds from the Toluk and Tabylgaty areas. (a, b) Site-mean directions of component B from the Toluk (squares) and Tabylgaty (circles) areas in situ (a) and after tilt correction (b). Stars are the locality-mean directions of component B with confidence circles (thick lines). (c–e) Endpoint directions of component C (triangles) and the segments of remagnetization circles for different sites from the Tabylgaty area after tilt correction. Diamonds are the site-mean directions of component C with confidence circles (thick lines); these means were computed by combining component directions and remagnetization circles after (McFadden and McElhinny, 1988). (f, g) Site-mean directions of component C from the Toluk (squares) and Tabylgaty (circles) areas in situ (f) and after tilt correction (g). Thick and thin dotted lines in (g) denote mean inclination and its confidence limits, respectively, computed with the aid of inclination-only statistics (McFadden and Reid, 1982). Solid (open) symbols and solid (dashed and dotted) lines are projected onto lower (upper) hemisphere.

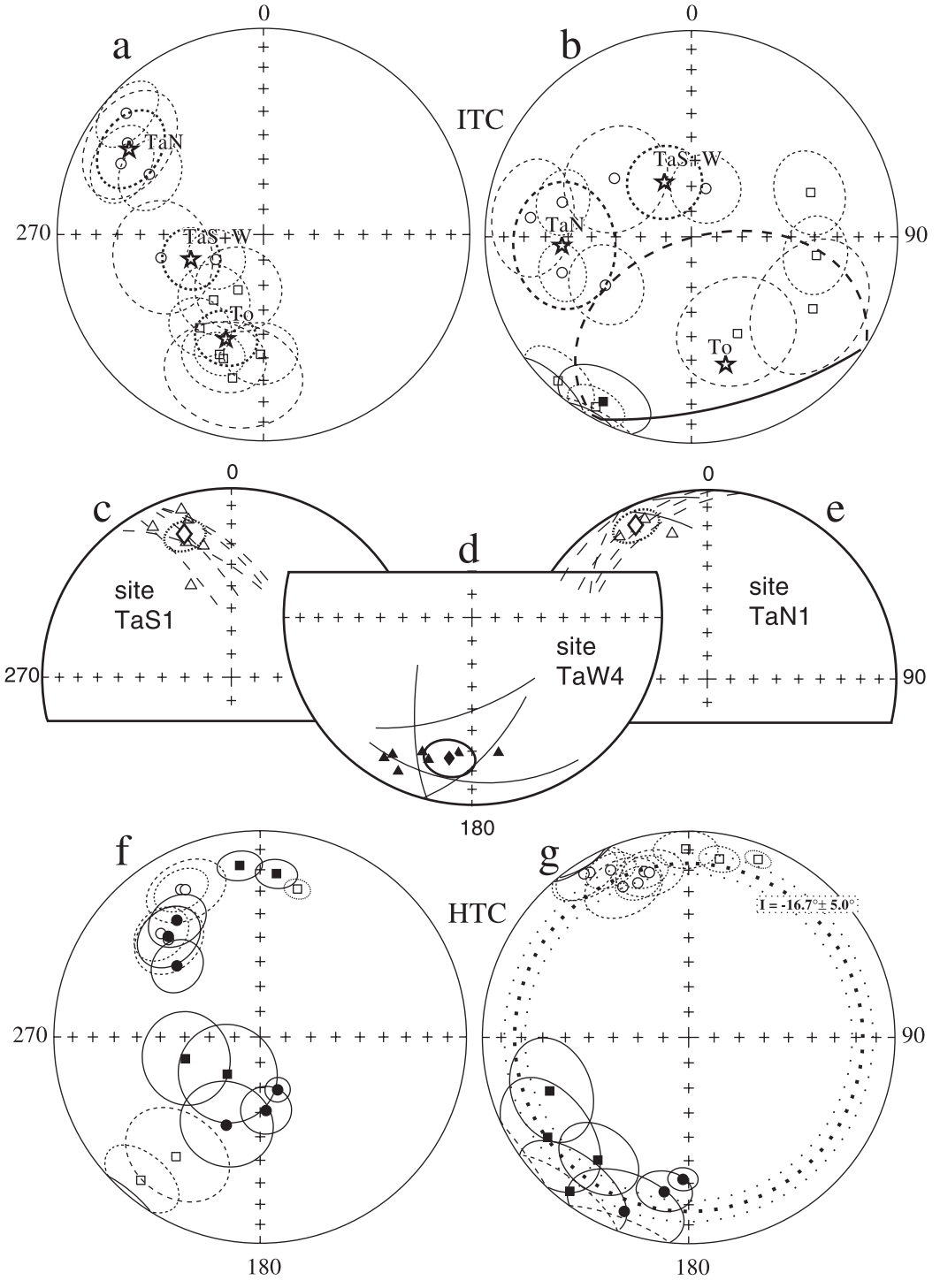
a
b
ITC
TaN
TaS+W
To
0
270
90
180
c
d
e
site
TaS1
site
TaW4
site
TaN1
f
g
HTC
I = -16.7 ± 5.0°

Table 2
Mean directions of component C in Upper Caradocian rocks from the Toluk and Tabylgaty areas

S/L	Data	N	B	In situ				Tilt-corrected			
				D (°)	I (°)	k	α_{95} (°)	D (°)	I (°)	k	α_{95} (°)
Toluk area											
ToR1	m	16/10	81/47	220.1	−29.8	7	19.2	222.7	6.4	8	18.6
ToR2	m	13/12	73/73	358.2	17.4	38	7.2	4.1	−9.5	21	9.7
ToR3	m	9/7	72/42	224.8	−10.5	22	13.1	221.5	26.9	18	14.7
ToR4	m	9/9	70/60	10.7	21.5	58	6.9	14.8	−13.2	68	6.4
ToR5*	m	14/10	248/55	226.5	70.4	7	19.5	239.7	17.3	7	20.4
ToR6	f	15/13	253/29	19.1	−26.9	86	4.5	26.3	−8.1	102	4.1
ToR7	m	17/5	248/30	258.8	59.0	20	17.9	253.9	28.6	19	18.3
INCL		(6)		–	−2.0	<3	54.1	–	−15.7	48	10.8
Tabylgaty area											
TaS1	m	11/11	234/48	321.2	−31.1	21	10.5	346.8	−22.2	39	7.6
TaS2	m	12/11	250/37	336.7	−19.9	25	9.3	350.0	−17.9	36	7.7
TaS3	m	9/9	221/37	321.7	−35.4	16	13.3	341.4	−21.4	16	13.3
TaS4	m	8/8	252/36	338.1	−21.0	18	13.7	351.6	−18.9	27	11.0
TaS		(4/4)		324.9	−27.1	52	12.8	342.5	−20.2	302	5.3
TaN1	m	11/8	29/66	329.5	31.1	31	10.7	340.0	−11.5	54	8.1
TaN2	m	10/7	16/59	322.6	34.3	34	12.1	334.1	−7.5	38	11.3
TaN3	m	12/8	4/65	315.5	45.9	37	10.3	332.4	−6.5	34	10.7
TaN4*	m	10/6	327/60	330.9	38.2	12	23.0	330.3	−21.3	11	25.2
TaN		(4/3)		323.0	37.2	72	14.6	335.5	−8.5	292	7.2
TaW1	m	11/8	204/41	206.0	52.2	12	17.6	205.3	11.0	11	18.5
TaW2	g	11/9	202/39	166.7	68.0	–	4.9	187.3	31.7	–	5.2
TaW3*	m	10/5	210/38	272.6	72.3	12	27.9	231.2	41.7	12	28.7
TaW4	m	13/11	209/38	180.4	60.7	24	9.7	194.0	25.2	25	9.4
TaW		(4/3)		187.2	61.3	41	19.5	196.0	22.8	36	20.8
INCL		(10)		–	−17.7	<3	41.0		−17.4	49	7.0
Overall mean											
INCL		(17)		–	−14.9	<3	27.6	–	−16.7	48	5.0

INCL, the inclination-only statistics is used (McFadden and Reid, 1982). Data, the type of data used: f, mean vector for direct observations (Fisher, 1953); m, mixed direct observations and remagnetization circles (McFadden and McElhinny, 1988); g, only remagnetization circles were used. Other notations as in Table 1.

*Rejected because of $\alpha_{95}>20°$.

before tilt correction in the others (component A) (Fig. 6g). Also numerous are the samples where these components have overlapping unblocking spectra, and hence large directional scatter is observed and only remagnetization circles could be used. Clustered directions of component B could be obtained from site TaW2 (Table 1). As a rule, high-temperature (C) components could only be isolated from lightly overprinted samples.

A rectilinear decay to the origin was observed in just a few samples from locality TaN (Fig. 6h). Usually, a component with in situ direction close to the present-day field (component A) is rather strong here, and, after its removal, component B with in situ negative inclination and westerly declination is often isolated (Fig. 6i). Acquisition of a strong spurious remanence around 600 °C because of mineralogical alteration prevented further cleaning of most samples. In just a few cases, something like an initial part of the final demagnetization segment could be observed (Fig. 6j); such "cluster means" are close to isolated directions of component C (Fig. 6h) and were used for further analysis.

The overall mean of component A ($D/I=353°/64°$, $\alpha_{95}=5°$) is close to the present-day dipole field ($D/I=0°/61°$). The mean directions of component B at localities TaS and TaW are similar in situ and more dispersed after tilt correction, while component B at

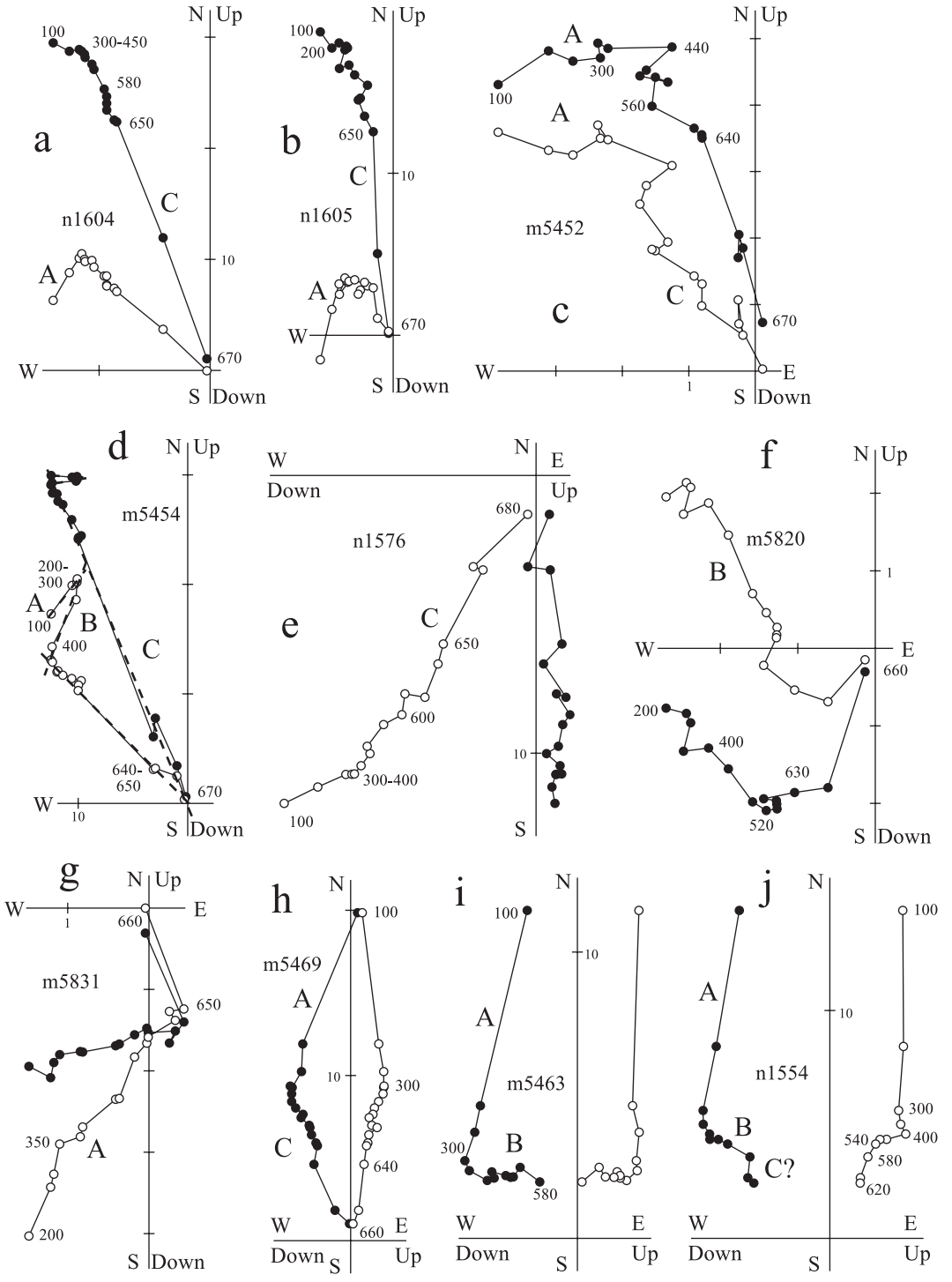

Fig. 6. Representative thermal demagnetization plots of Ordovician rocks from the Tabylgaty area (a–d, locality S; e–g, locality W; h–j, locality N) in stratigraphic coordinates. Other notations as in Fig. 4.

locality TaN differs both in declination and inclination (Fig. 5a,b; Table 1).

Component C persists above 650 °C implying hematite as the carrier. It is reliably isolated from more than half of samples at locality TaS, but the site means include data from remagnetization great circles (Fig. 5c). On average, this component is isolated from fewer samples at the other two localities, and the site means are based on more remagnetization circles (Fig. 5d,e). Because of the presence of two overprints, two remagnetization circles are often recognized, and the higher-temperature circles were used for calculation of component C. If only one remagnetization circle is observed, it was used only if the magnetization persists above 500 °C.

The means for localities TaS and TaN point to the northwest and shallowly upward and to the southwest and downward at locality TaW (Table 2; Fig. 5g), indicating that two polarities are present, although they are not antipodal. Bedding attitudes at each locality are rather uniform, and a fold test can be performed only for the three localities combined. The inclination-only fold test (McFadden and Reid, 1982) is positive for 10 site means from three localities (Table 2), and the minimal dispersion of inclinations is observed at 100% unfolding. In Section 5, we will return to the issue of the non-antipodal declinations.

4.1.3. West Kyrgyz Range

A low-temperature component in Lower Caradocian redbeds of the Almaly Fm. is removed by heating up to 350 °C (Fig. 7a,b). Data grouping decreases significantly upon tilt correction, and the mean direc-

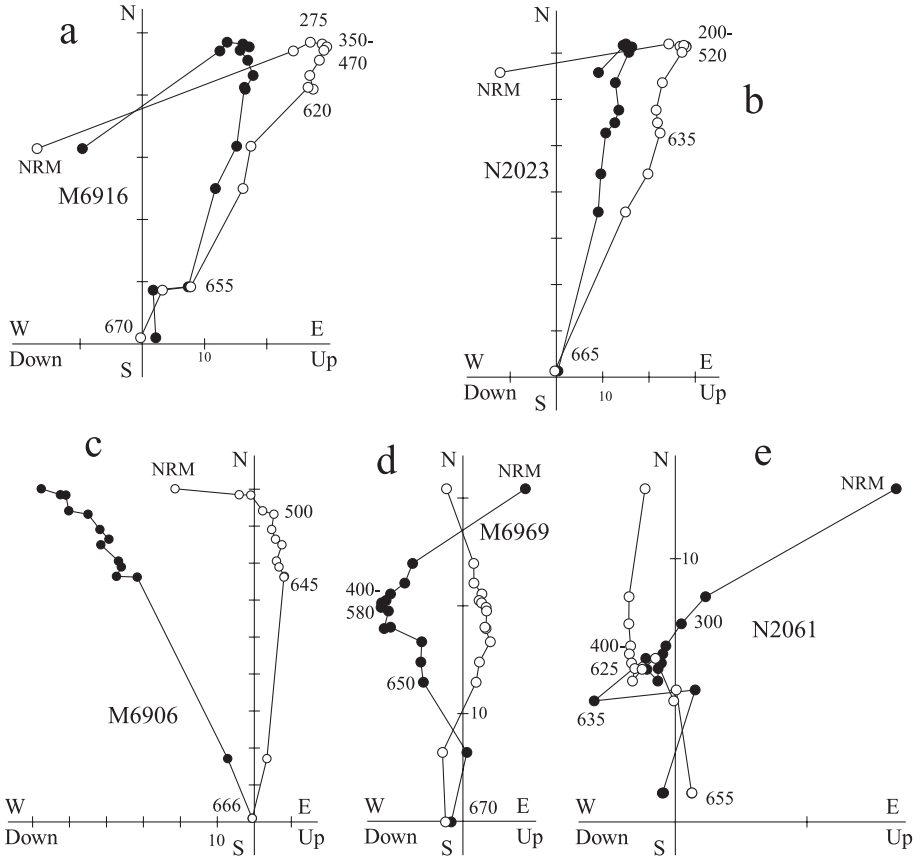

Fig. 7. Representative thermal demagnetization plots of Lower Caradocian (a, b) and Ashgillian (c–e) rocks from the West Kyrgyz Range in stratigraphic coordinates. Other notations as in Fig. 4.

tion of this component in situ is close to that of the present-day field for the study area. Hence, the low-temperature component is a recent overprint. After its removal, both direction and intensity of remanent magnetization do not change over a temperature interval of 150 °C to more than 300 °C. At higher temperatures, a linear decay to the origin is observed in most samples, and a high-temperature component (HTC) is reliably isolated (Fig. 7a,b). An adequate isolation of the HTC is not achieved in just a few samples, and remagnetization circles are combined for calculation of site-mean directions.

Two sites were rejected because of unstable behavior during cleaning and high scatter, but HTC site-mean directions are well defined for the remaining 13 sites (Table 3). Upon tilt correction, site means show statistically significant improvement in grouping (Fig. 8a,b); although the maximum k is 118 for 85% unfolding, this value is statistically indistinguishable from that for 100% unfolding ($k=110$), and we conclude that the HTC is prefolding.

During demagnetization, Ashgillian redbeds from the southern locality (sites AS1 to AS4, Fig. 3c) behave similarly to Lower Caradocian rocks in that a recent overprint and an HTC can be isolated (Fig. 7c). Unblocking temperatures of the former, however, extend to higher temperatures; as a result, more samples give only remagnetization circles. Despite this, the four site means are well defined and group better, but not significantly so, upon tilt correction (Table 4, South).

In a few Ashgillian samples from the northern locality (sites AS5 to AS11, Fig. 3c), an HTC can be isolated after removal of a recent overprint, but the data are noisier and this overprint appears to have higher unblocking temperatures (Fig. 7d). Most samples, however, acquire strong spurious remanence at, or slightly above, 620 °C, thus preventing proper HTC isolation (Fig. 7e). Remagnetization circles can be identified in relatively few cases. As a result, only three sites give adequately defined mean directions (Table 4, North). Unfortunately, no HTC could be isolated from 20 pebbles of Ashgillian redbeds within the Visean basal conglomerate.

HTC site means in Ashgillian rocks have very shallow inclinations and northwesterly declinations, which, coincidentally, are nearly parallel to the strike at the northern locality, and hence tilt correction does not lead to a significant change in data grouping. Moreover, the mean HTC directions for two localities (=two limbs) are statistically different for both in situ and corrected data, the values of F statistics of 8.65 and 7.01, respectively, exceeding the 95% critical value of 4.10 (McFadden and Jones, 1981).

Visean rocks dip 0°/23° at the northern locality, while the bedding of Ashgillian redbeds below the angular unconformity is about 75°/75°. Thus we have an opportunity to correct for two deformation stages

Table 3
High-temperature component from the Lower Caradocian rocks (Almaly Fm.) of the West Kyrgyz Range

Site	N	B	In situ				Tilt-corrected			
			D (°)	I (°)	k	α_{95} (°)	D (°)	I (°)	k	α_{95} (°)
LI	7/4	305/38	26.0	−21.5	64	11.5	41.2	−21.6	162	7.2
L2	10/10	287/50	21.7	−29.4	28	9.3	43.1	−15.3	52	6.8
L3	10/10	235/35	20.3	−43.6	50	6.9	30.0	−13.0	48	7.1
L4	6/5	219/38	33.8	−60.9	28	15.1	36.5	−22.9	27	15.5
L5	6/6	226/38	15.4	−47.9	29	12.8	25.3	−13.4	75	7.8
L6	6/6	215/46	26.3	−65.7	30	13.2	31.4	−19.5	37	12.0
L7	7/7	218/50	8.1	−61.4	37	10.2	23.9	−14.7	32	11.0
L8	7/7	248/41	6.5	−49.5	50	8.8	30.1	−21.9	113	5.8
L9	8/7	227/40	23.5	−49.0	72	7.4	31.6	−10.9	72	7.4
L10	10/8	228/48	7.5	−56.4	66	6.9	26.4	−14.6	111	5.3
L11	10/8	233/41	12.5	−49.0	16	14.6	26.9	−14.4	37	9.4
L12	10/8	234/51	0.6	−58.6	61	7.2	27.5	−17.0	70	6.7
L13	8/8	215/38	27.6	−68.0	39	9.8	31.8	−30.1	39	9.8
Mean	15/13		17.8	−51.3	30	7.6	31.1	−17.7	110	4.0

Notations as in Table 1.

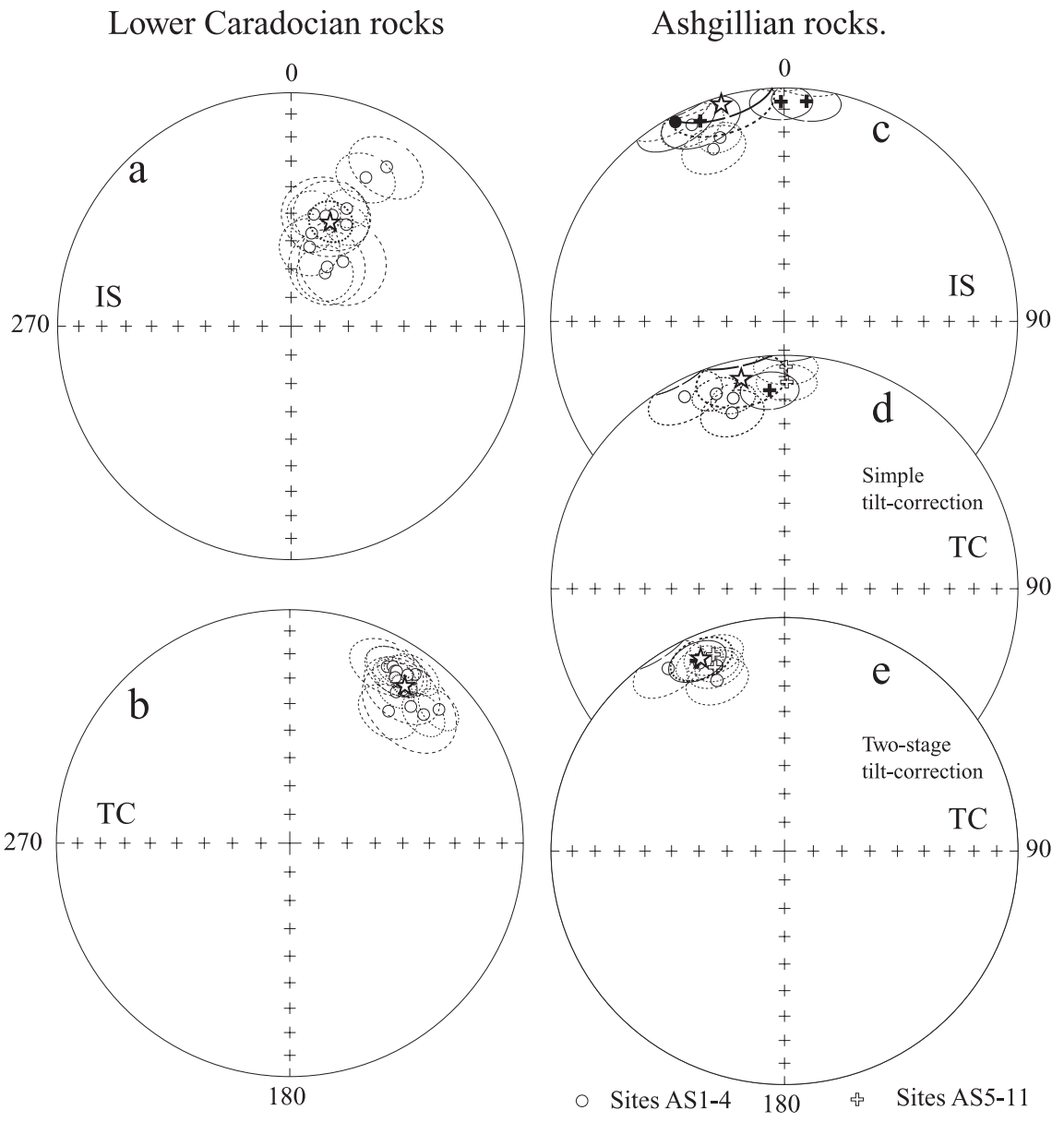

Fig. 8. Stereoplots of site-mean directions of the HTC from Lower Caradocian (a, b) and Ashgillian (c–e) rocks from the West Kyrgyz Range with confidence circles (thin lines) in situ (a, c) and after tilt correction (b, d, e). Other notations as in Fig. 5.

separately; the algorithm is similar to that commonly used for two-stage correction for a fold with plunging axis. After this correction, the value of F statistics drops to 1.19, which is certainly insignificant. Hence, the fold test of McFadden and Jones (1981) becomes clearly positive with this two-stage correction.

4.1.4. Combined Ordovician data

The redbeds studied at the Toluk and Tabylgaty areas are of similar Late Caradocian age, and their pooling is justified. For the combined data set, the scatter of site means in situ is very large (Fig. 5f), whereas the site means form two non-antipodal polar-

Table 4
High-temperature component from the Ashgillian rocks (Botmoynak Fm.) of the West Kyrgyz Range

Site	*N*	B	In situ				Tilt-corrected			
			D (°)	*I* (°)	*k*	α_{95} (°)	*D* (°)	*I* (°)	*k*	α_{95} (°)
AS1	5/5	251/27	326.4	3.1	50	10.9	327.5	− 8.1	54	10.5
AS2	5/5	241/32	329.8	− 7.7	77	8.8	335.7	− 12.5	126	6.8
AS3	7/7	240/14	332.7	− 21.3	43	9.6	338.4	− 22.4	45	9.4
AS4	7/7	233/13	335.8	− 17.7	102	6.2	339.9	− 16.6	96	6.3
South	(4/4)		331.1	− 11.0	49	13.3	335.3	− 15.0	99	9.3
AS5	10/10	75/72	354.2	6.5	39	8.2	355.3	− 5.4	38	8.3
							340.1	*− 11.4*		
AS6	10/10	77/78	0.8	5.8	30	9.0	355.6	− 12.4	36	8.2
							339.3	*− 17.0*		
AS10	12/9	77/75	332.3	7.7	24	10.9	350.7	15.8	42	8.2
							335.3	*11.3*		
North	(7/3)		349.2	6.8	30	22.9	353.9	− 0.7	30	23.1
							338.2	*− 5.8*	*29*	*23.5*
Mean	(11/7)		338.8	− 3.4	21	13.6	343.4	− 9.0	25	12.2
							336.6	*− 11.1*	*48*	*8.8*

South and North are for two Ashgillian localities (Fig. 3c). Italicized are the data for two-stage tilt correction for the north locality (see text for detail). Other notations as in Table 1.

ity groups after tilt correction (Fig. 5g). Some rotation between the two study areas is indicated by clockwise displacement of the Toluk directions (squares) with respect to the Tabylgaty data (circles in Fig. 5g). The inclination-only fold test (McFadden and Reid, 1982) is positive for the entire data set, and the best data grouping is achieved at 100% unfolding.

A disturbing feature, however, is that the directions of the two polarities are not antipodal, the difference being mainly in declination (Fig. 5g). Also important is the fact that southwesterly directions are clockwise rotated with respect to the northerly ones for both the Tabylgaty and Toluk data sets and for each limb of the Toluk data as well. A local rotation may account for difference between the Toluk and Tabylgaty data, but it cannot be invoked to explain the site-mean directions of the Toluk area's west limb (ToR1–4), which come from a locality with a fairly coherent structure. The imperfect antipodality may reflect asymmetric reversals as has previously been suggested for the Ordovician field (Torsvik et al., 1995). On the other hand, this pattern could also result from somewhat different ages of magnetization or from incomplete removal of a secondary remanence, which has to lie on the great circle through the polarity groups and hence must have shallow inclination too. As the folding of the Ordovician rocks in the NTZ is certainly of pre-Early Devonian age and most likely occurred close to the Ordovician–Silurian boundary as discussed above, the direction of the remagnetizing field is likely to be close to one of the two polarity groups. For instance, a remagnetization might have taken place in the Ashgillian, as the Ashgillian mean direction (Table 4; Fig. 8e) is identical to the northwesterly directions of Fig. 5g. Tentatively, this overprinting can be connected with large granite bodies of Late Ordovician age, which cut through the entire lower Paleozoic section (Fig. 2). If so, incomplete removal of the overprint has not much distorted the true inclination in Upper Caradocian redbeds, and this overprint is largely cancelled when the sum of all data is used. The three mean Late Ordovician inclinations (− 17.4°, − 17.7°, and − 11.1°; Tables 2–4) are reassuringly similar.

Thus the positive inclination-only fold test, the presence of two polarities, and the sharp difference of component C directions from the ITC and HTC in Carboniferous rocks both in situ and after tilt correction (see below) imply an Ordovician age of the high-temperature components in the Toluk and Tabylgaty redbeds. Early Caradocian and Ashgillian results from the West Kyrgyz Range are also supported by the fold test. In both cases, the deformation the fold test is based on is entirely or largely of pre-Carboniferous age and most likely occurred close to the Ordovician–Silurian boundary. Hence the prefolding nature of the

HTCs in all three collections is synonymous to them being near-primary.

4.2. Carboniferous rocks

4.2.1. Visean–Serpukhovian redbeds of the Tabylgaty area (Dungurma Fm.)

At localities CA and CC, no stable remanence was found in some samples above 300 °C. In the other samples, a scattered unstable component of varying intensity is removed below 300 °C, and, then, a single component persists to well above 600°, sometimes to 680 °C (Fig. 9a–c). This rather dispersed component (Table 5) does not generally decay to the origin and indicates that another remanence is present in these rocks. The high-temperature component isolated from just a few samples (Fig. 9c,d) is very scattered and cannot be used.

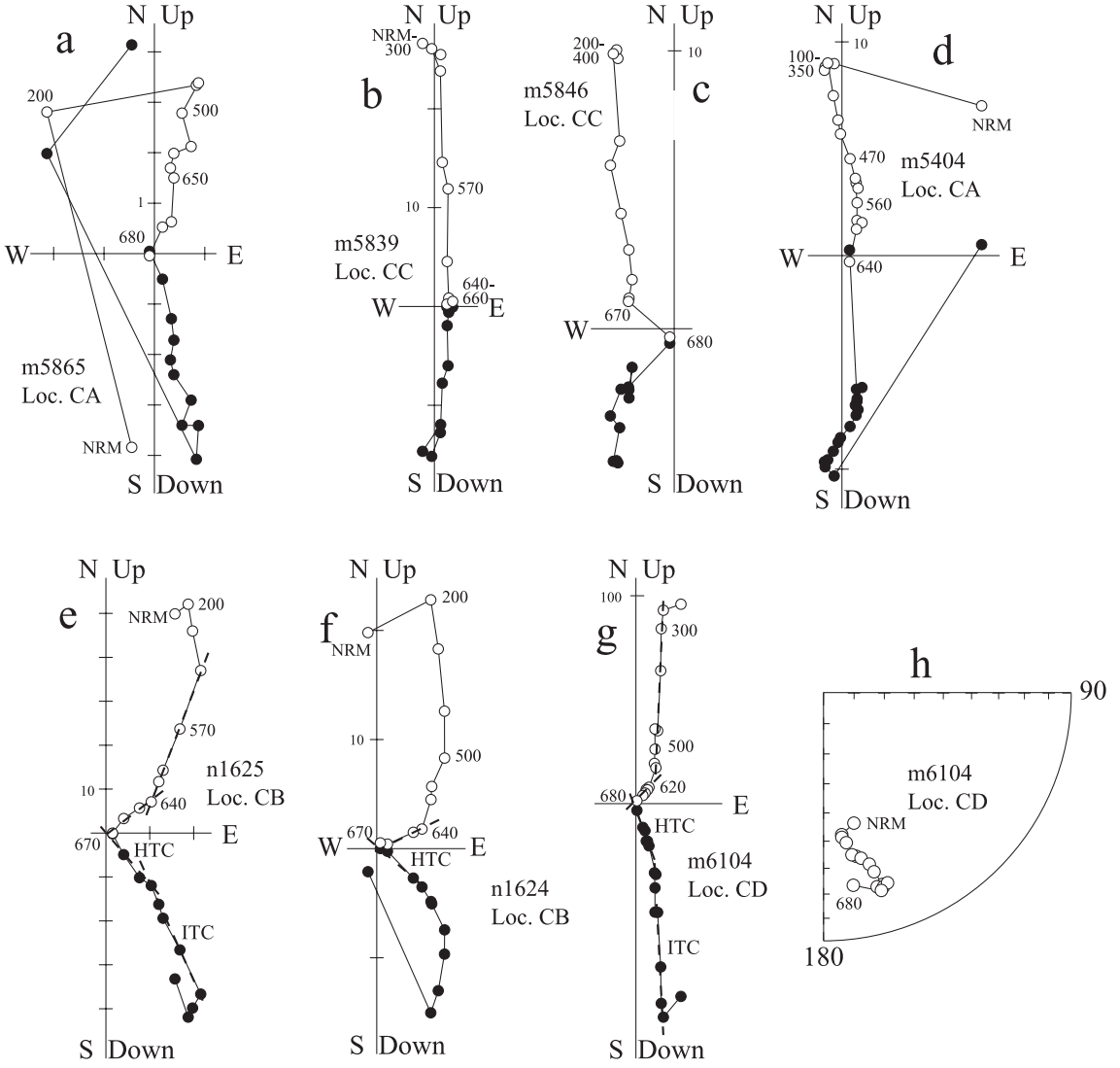

Fig. 9. Representative thermal demagnetization plots of Lower Carboniferous rocks from the Tabylgaty area (Dungurma Fm.) in stratigraphic coordinates; the localities of the samples (CA–CE) are indicated. Other notations as in Fig. 4.

Table 5
Mean ITC directions in Lower Carboniferous redbeds of the Tabylgaty area (Dungurma Fm.)

S/L	N	B	In situ				Tilt-corrected			
			D (°)	I (°)	k	α_{95} (°)	D (°)	I (°)	k	α_{95} (°)
CA1*	6/6	136/46	166.9	−42.5	10	22.9	234.9	−70.9	10	22.4
CA2	13/12	134/41	158.9	−30.3	10	14.5	185.8	−66.1	8	16.1
CB1	7/6	358/37	106.4	−81.8	58	8.9	170.8	−50.9	47	9.9
CB2	6/6	1/39	90.6	−77.7	118	6.2	166.6	−50.3	132	5.9
CB3	7/7	0/41	48.9	−85.7	92	6.3	179.9	−51.8	114	5.7
CB4	7/7	8/41	83.2	−77.3	70	7.3	173.4	−52.0	96	6.2
CB5	6/6	2/40	81.7	−72.7	306	3.8	159.7	−51.6	261	4.2
CB6	7/6	4/41	90.6	−73.3	46	9.9	163.8	−48.8	45	10.1
CB	(6/6)		86.5	−78.3	205	4.7	168.9	−51.1	299	3.9
CC1	11/10	199/32	209.2	−32.7	13	13.9	214.1	−64.3	16	12.6
CC2	13/6	192/33	195.6	−28.7	13	19.4	186.6	−60.6	24	14.1
CC3	9/6	181/29	187.9	−17.3	24	14.0	188.7	−46.7	23	14.1
CC	(3/3)		197.1	−26.5	42	19.2	194.8	−57.7	46	18.5
CD1	6/6	33/53	83.9	−66.1	77	7.7	190.0	−50.9	126	6.0
CD2	6/6	30/52	88.7	−69.4	46	10.0	190.1	−48.3	122	6.1
CD3	6/6	33/55	90.7	−64.6	208	4.7	188.0	−46.6	301	3.9
CD4	7/7	33/55	93.2	−60.5	206	4.2	181.5	−47.0	182	4.5
CD5	6/6	33/54	92.2	−62.7	115	6.3	184.7	−47.4	183	5.0
CD	(5/5)		90.0	−64.7	472	3.5	186.8	−48.1	720	2.9
CE1**	4/4	189/67	223.0	1.0	187	6.7	244.2	−59.8	94	9.5
CE2	6/6	187/51	202.6	8.6	121	6.1	206.0	−41.7	90	7.1
CE3	5/5	188/39	196.3	−2.0	71	9.2	197.4	−41.0	192	5.5
CE4	5/5	193/46	201.3	5.9	87	8.3	202.3	−39.6	210	5.3
CE	(3/3)		200.1	4.2	157	9.9	201.9	−40.8	570	5.2
A+C	(5/4)		183.0	−28.4	17	22.8	188.0	−59.9	56	12.4
B+D+E	(15/14)		139.6	−70.6	4	22.8	183.3	−48.6	59	5.2
MEAN	(20/18)		163.0	−62.1	4	20.5	185.0	−51.1	49	5.0
INCL	(20/18)			−64.3	>3	25.7		−50.9	63	4.3

S/L, sites (with numerical) and localities labeled as in the text and Fig. 3b; A+C, mean for localities CA and CC; B+D+E, mean for localities CB, CD, and CE. Other notations as in Table 1.

*Rejected because of $\alpha_{95}>20°$.

**Not used (see text).

At localities CB, CD, and CE, after removal of a weak scattered remanence at 200–300 °C, the NRM consists of intermediate- (ITC) and high-temperature (HTC) components (Fig. 9e–g). The ITC persists from 300 to 600–640 °C and is represented in most samples by linear segments which clearly miss the origin; a few samples display curved trajectories in the 300–600 °C interval (Fig. 9f). After removal of this component, the HTC can be reliably isolated from most samples. Even when the HTC is weak (Fig. 9g), its presence is confirmed by short but well-defined remagnetization circles (Fig. 9g–h).

The within-site dispersal of the ITC and HTC is low, and all site means are well defined (Tables 5 and 6). The site means are scattered in situ and tightly grouped after correction for tilt, except for site CE1 (Tables 5 and 6; Fig. 10). This site is from a structurally disturbed outcrop, and the ITC and HTC directions are both anomalous with respect to the other data; hence we excluded this site from further analysis.

Demagnetization properties of the samples from localities CA and CC on one hand, and localities CB, CD, and CE on the other, are rather different, and it is not self-evident that the only component from the former and the ITC from the latter are of the same age. These remanences persist from 200–300 to above 600 °C and do not show a rectilinear decay to the origin, being overprints. For each component, the best data grouping is reached at, or close to, 100% unfolding,

Table 6
Mean HTC directions in Lower Carboniferous redbeds of the Tabylgaty area (Dungurma Fm.)

S/L	N	B	In situ				Tilt-corrected			
			D (°)	I (°)	k	α_{95} (°)	D (°)	I (°)	k	α_{95} (°)
CB1	7/6	358/37	122.9	− 64.9	49	9.7	155.6	− 37.0	36	11.4
CB2	6/6	1/39	114.0	− 62.3	61	8.7	152.6	− 36.4	59	8.8
CB3	7/6	0/41	124.6	− 69.3	68	8.2	162.1	− 36.3	79	7.6
CB4	7/7	8/41	112.9	− 57.8	48	8.8	152.9	− 35.5	51	8.6
CB5	6/6	2/40	104.5	− 53.3	37	11.2	141.3	− 34.6	38	10.9
CB6*	7/6	4/41	111.9	− 55.2	55	9.5	147.6	− 32.5	86	7.6
CB	(6/6)		114.0	− 60.6	132	5.9	151.9	− 35.5	183	5.0
CD1	7/6	33/53	123.3	− 46.1	48	9.7	163.9	− 27.9	38	11.0
CD2	6/5	30/52	127.3	− 47.5	56	10.3	167.8	− 26.8	46	11.5
CD3	6/6	33/55	124.6	− 52.0	101	6.7	173.6	− 28.5	68	8.2
CD4	7/7	33/55	124.8	− 39.1	55	8.2	159.3	− 21.9	51	8.5
CD5	6/5	33/54	127.1	− 40.2	24	15.9	162.2	− 23.5	35	13.1
CD	(5/5)		125.5	− 45.0	219	5.2	165.2	− 25.8	199	5.4
CE1**	4/4	189/67	223.1	9.1	56	12.3	235.8	− 52.4	29	17.3
CE2	6/6	187/51	187.1	21.3	38	11.0	186.5	− 29.5	51	9.5
CE3	5/5	188/39	183.1	8.0	32	13.6	182.0	− 30.2	40	12.3
CE4	5/5	193/46	186.8	18.7	44	11.7	186.1	− 26.2	62	9.8
CE	(4/3)		185.6	16.0	121	11.3	184.9	− 28.7	699	4.7
MEAN	(15/14)		139.2	− 44.5	5	20.4	164.1	− 31.2	39	6.4
INCL	(15/14)			− 38.5	3	14.7		− 30.7	132	3.4

INCL, the inclination-only statistics is used (McFadden and Reid, 1982). Other notations as in Tables 1 and 2.
* Direct observations and remagnetization circles are combined.
** Not used (see text).

and their mean directions differ insignificantly (Table 5). We think that the same component is isolated everywhere, so that the data can be pooled. The best data grouping for all 18 sites is reached at 100% unfolding; hence this remanence is a prefolding overprint. The inclination-only fold test (McFadden and Reid, 1982) is also positive for the HTC data, and site-mean inclinations are also best grouped at 100% unfolding. Therefore, this component is prefolding too. At the same time, a difference of $20 \pm 4°$ between mean ITC and HTC inclinations is observed; also the differences between ITC and HTC declinations at each locality are statistically similar and are about 20° on average. These results indicate that these remanences are of different ages.

The ITC and HTC data from localities CB, CD, and CE show a banana-type distribution in stratigraphic coordinates, mostly because of the statistically significant differences between locality mean declinations (Fig. 10b,d; Tables 5 and 6). The dip azimuths, however, do not correlate with paleomagnetic declinations. Thus deformation of Carboniferous rocks which led to this elongation cannot be unraveled without a lot of additional and detailed sampling.

The Lower Carboniferous Dungurma redbeds might have been deformed during thrusting in Bashkirian time, but the purely prefolding nature of the ITC in these rocks and the assumed substantial difference in ages of the ITC and HTC indicate that this deformation did not affect the Tabylgaty area north of the thrust (Fig. 3b). The next folding in the NTZ took place in the latest Permian–Triassic (Fig. 2), and both the ITC and HTC predate this deformation. As these remanences are ubiquitously reversed, they are likely to have been acquired before the end of the Kiaman superchron, i.e. in pre-Tatarian time (Opdyke and Channell, 1996). We make the common assumption that a component with the higher unblocking temperatures is the older, and hence the HTC is an older and most probably primary remanence in the Dungurma redbeds. As will be discussed below, the northward movement of the area during the Paleozoic, as seen in the inclinations, is additional evidence for the relative age assignments of the ITC and HTC.

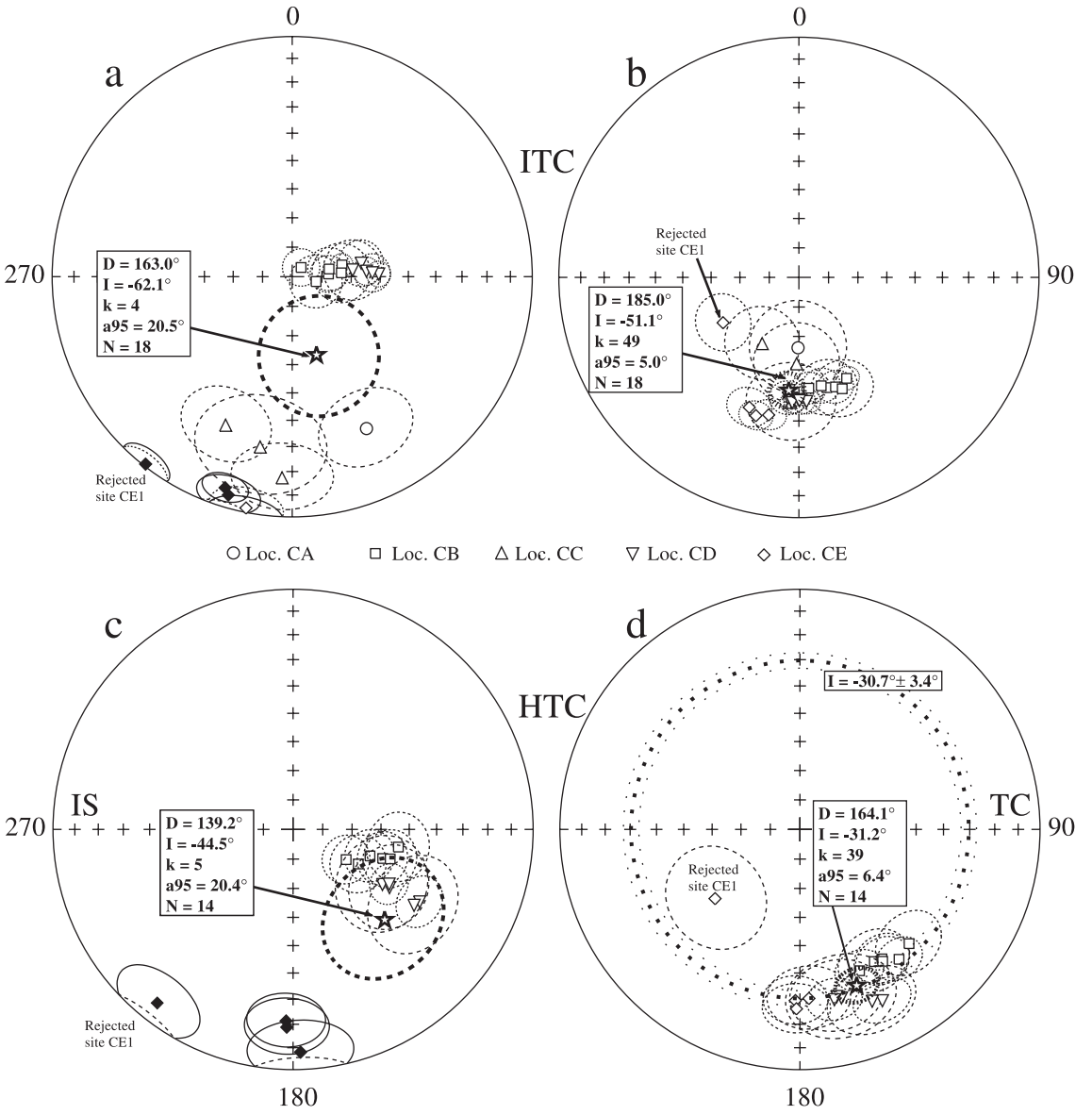

Fig. 10. Stereoplots of ITC (a, b) and HTC (c, d) site-mean directions with confidence circles (thin lines) in Lower Carboniferous redbeds of the Dungurma Fm. in situ (a, c) and after tilt correction (b, d). The site means from different localities are distinguished by the different symbols as indicated in the middle of the figure. Stars are the overall mean directions of these components with confidence circles (thick lines). Thick and thin dotted lines in 'd' denote mean inclination and its confidence limits, respectively, computed with the aid of inclination-only statistics (McFadden and Reid, 1982). Other notations as in Fig. 5.

4.2.2. Bashkirian redbeds of the West Kyrgyz Range

After removal of a weak scattered remanence at 200–300 °C, some samples reveal a single component of reversed polarity that decays to the origin (Fig. 11a), while two components can be isolated from the others (Fig. 11b above 200 °C). An ITC from the bicomponent samples is always reversed and its directions are similar to those from single-component samples. We conclude that this remanence is an overprint but that the degree of overprinting varies

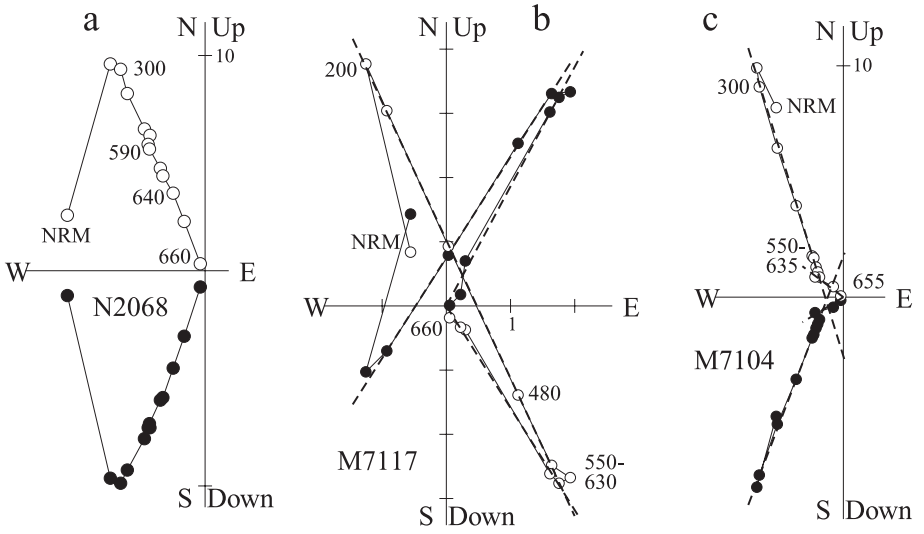

Fig. 11. Representative thermal demagnetization plots of Bashkirian rocks from the West Kyrgyz Range in stratigraphic coordinates. Other notations as in Fig. 4.

greatly. The overprint is isolated from most samples, and its site-mean directions are precisely defined at most sites (Table 7). Tilt correction many-fold decreases the data scatter (Fig. 12a,b), and the best grouping is observed after complete unfolding. Hence, this overprint is prefolding.

HTC is reliably isolated from about one third of the collection (Fig. 11c) and it has normal polarity everywhere but for one sample. Many samples revealed long well defined remagnetization circles, and site means were computed combining them with direct observations (McFadden and McElhinny, 1988). The HTC site means are statistically meaningful for 9 out of 12 sites studied (Table 8). Tilt-corrected data are significantly better grouped than those in situ (Fig. 12c,d); the best grouping occurs between 90% and 100% unfolding, the maximum concentration parameter being only a few percent larger than the fully tilt-corrected value. Hence, the HTC in Bashkirian redbeds is prefolding and, judging by its higher unblocking temperatures, older than the reversed ITC in the same rocks. Because Bashkirian

Table 7
Mean ITC directions from the Bashkirian (lower Middle Carboniferous) rocks of the West Kyrgyz Range

Site	*N*	B	In situ				Tilt-corrected			
			D (°)	*I* (°)	*k*	α_{95} (°)	*D* (°)	*I* (°)	*k*	α_{95} (°)
B1	10/10	324/21	227.4	− 59.6	82	5.4	198.1	− 51.7	82	5.4
B2	9/8	353/23	219.1	− 66.8	30	10.3	198.0	− 47.8	32	10.0
B3	9/9	359/21	218.6	− 69.4	69	6.3	199.5	− 50.7	55	7.0
B4	8/6	22/105	17.3	− 17.0	79	7.6	210.5	− 57.7	79	7.6
B6	7/7	50/20	204.4	− 58.5	10	20.0	212.5	− 40.7	11	19.0
B7	9/8	31/24	195.2	− 75.4	85	6.0	204.9	− 51.8	112	5.2
B8	7/7	23/20	200.8	− 72.6	180	4.5	202.1	− 52.6	142	5.1
B9	7/7	36/21	199.0	− 70.4	91	6.3	207.4	− 49.5	94	6.3
B10	7/7	176/23	196.4	− 27.9	193	4.4	204.1	− 49.0	155	4.9
B11	8/8	176/28	201.1	− 21.8	60	7.2	210.7	− 46.3	55	7.5
B12	7/7	167/14	195.5	−38.5	65	7.5	202.4	− 50.0	55	8.2
Mean	(12/11)		205.9	− 62.8	6	21.2	204.7	− 49.9	225	3.1

Sites are labeled as in Fig. 3c. Other notations as in Tables 1 and 2.

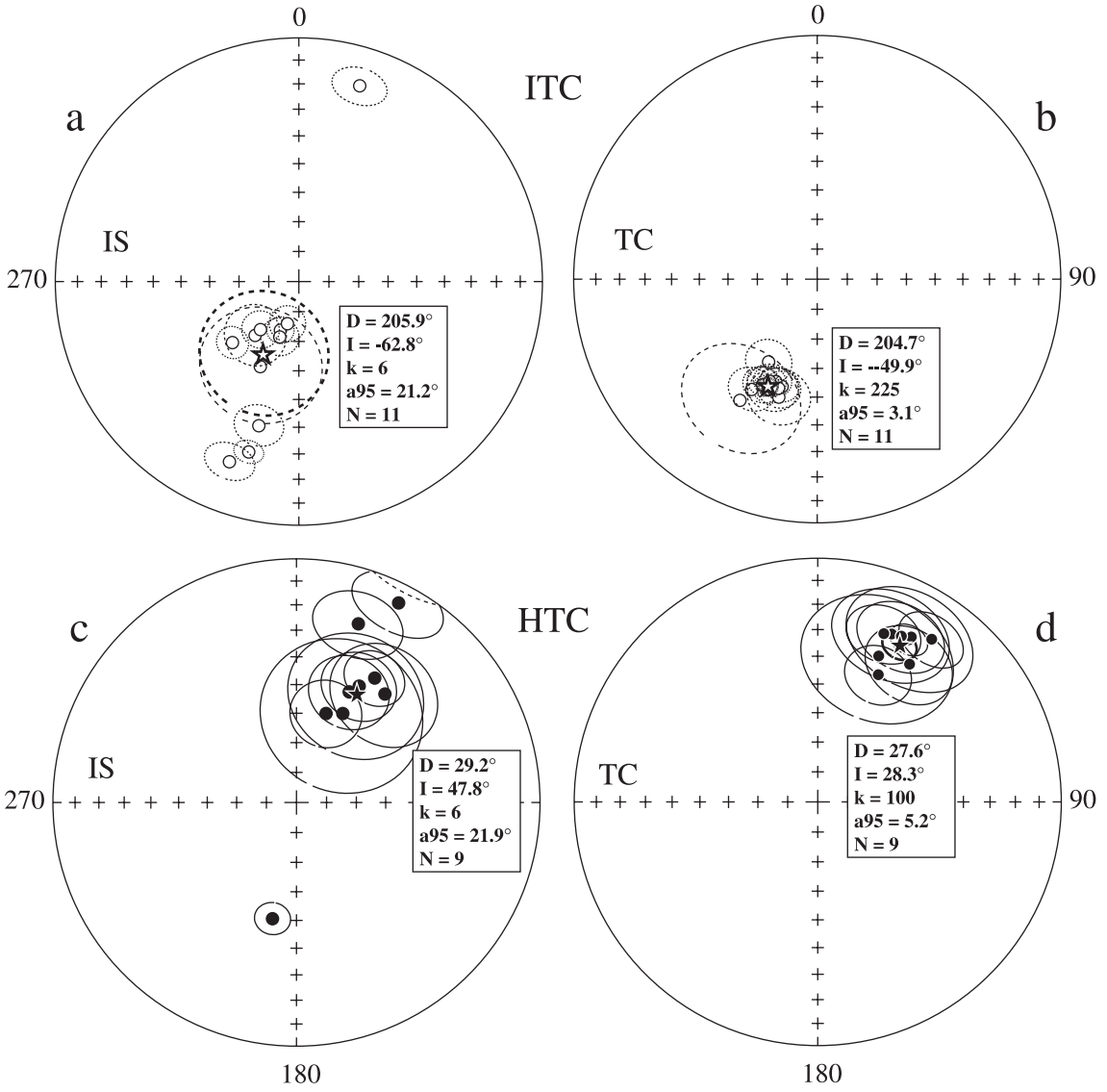

Fig. 12. Stereoplots of ITC (a, b) and HTC (c, d) site-mean directions (circles) with confidence circles (thin lines) in Bashkirian redbeds in situ (a, c) and after tilt correction (b, d). Stars are the overall mean directions of these components with confidence circles (thick lines). Other notations as in Fig. 5.

time is close to the base of the Kiaman (Opdyke et al., 2000), this remanence is primary.

4.3. Overprint data

The tilt-corrected ITCs in the Lower Carboniferous and Bashkirian rocks, and the in situ component B direction from the Toluk area are of reversed polarity and have different declinations but similar inclinations (Fig. 13). This agreement in inclinations and polarity gives ground to assume a similar age of the above remanences and to calculate their overall mean with the aid of inclination-only statistics (McFadden and Reid, 1982). The overall mean inclination agrees with, and falls between, the Early and Late Permian, but differs from the Late Carboniferous and Early Triassic,

Table 8
Mean HTC directions from the Bashkirian (lower Middle Carboniferous) rocks of the West Kyrgyz Range

Site	*N*	B	In situ				Tilt-corrected			
			D (°)	*I* (°)	*k*	α_{95} (°)	*D* (°)	*I* (°)	*k*	α_{95} (°)
B2	9/6	353/23	39.2	42.1	19	17.6	29.6	23.2	16	18.9
B3	9/6	359/21	28.3	44.9	35	12.0	21.5	26.7	41	11.0
B4	8/7	22/105	191.7	49.7	115	5.7	29.3	24.7	115	5.7
B6	7/3	50/20	32.2	39.5	227	9.6	35.0	19.6	224	9.7
B7	9/5	31/24	25.5	48.3	46	12.9	26.8	24.8	46	13.0
B8	7/3	23/20	27.5	56.2	31	26.6	22.7	35.4	40	23.4
B9	7/6	36/21	18.4	58.4	39	11.6	25.5	42	48	10.5
B11	8/6	176/28	27.1	8.8	37	12.5	33.7	32.6	31	13.7
B12	7/7	167/14	19.1	23.4	29	13.0	23.8	25.7	17	17.3
Mean	(12/9)		29.2	47.8	6	21.9	27.6	28.3	100	5.2

Sites are labeled as in Fig. 3c. Other notations as in Tables 1 and 2.

reference directions recalculated to the North Tien Shan (41.8°N, 73.8°E) from the corresponding poles of Baltica (Van der Voo, 1993). The overall mean inclinations also agree well with Permian paleomagnetic data (Audibert and Bazhenov, 1992; Bazhenov et al., 1999) from two localities 100 to 150 km to the east

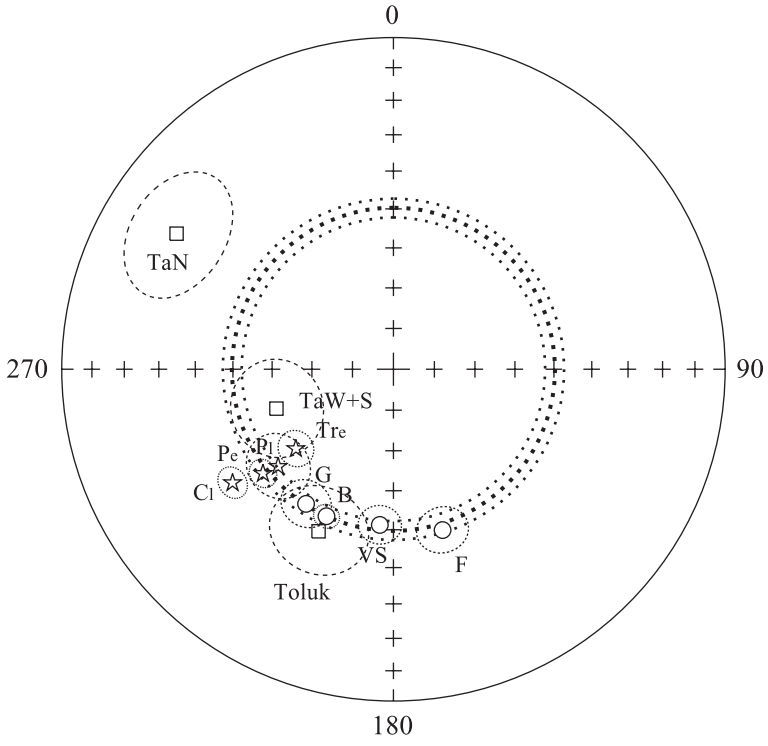

Fig. 13. Stereoplot of overprint mean directions and Permian data from the North Tien Shan and the European reference directions with associated confidence circles (thin dashed lines). VS and B, the ITC in the Visean–Serpukhovian and Bashkirian redbeds, respectively; F and G, locality-mean directions in Permian rocks of the North Tien Shan (Bazhenov et al., 1999); Toluk, overall mean of component B from the Toluk area; TaN and TaW + S, mean directions of component B from different localities in the Tabylgaty area; C_l, P_e, P_l, and Tr_e, Late Carboniferous, Early and Late Permian, and Early Triassic reference directions, respectively, recalculated from the data for the European platform (Van der Voo, 1993). Circles (squares) are in stratigraphic (geographic) coordinates. Thick dotted line is mean inclination (McFadden and Reid, 1982) for ITC results with associated confidence limits (dotted circles). All symbols are projected onto upper hemisphere.

from the Toluk area in the NTZ (F and G, Fig. 1b). Note also that mean declinations of the Permian and overprint directions are CCW rotated through various angles with respect to the late Paleozoic reference declinations (Fig. 13). These observations further confirm that CCW rotations affected most of the Tien Shan in latest Paleozoic to Triassic time, and that this belt did not move latitudinally with respect to Baltica (Bazhenov et al., 1999).

The mean direction of component B from localities TaS and TaW is somewhat steeper and CW rotated with respect to the Late Paleozoic reference declination, but the differences are barely significant (Fig. 13). Taking into account the limited number of samples where component B was isolated at these two localities, we assign a Permian age also to this remanence (but did not include it in further analyses). More deviating from the reference directions are both mean inclination and declination of component B from locality TaN (Fig. 13). This result is impossible to explain by either rotation around vertical axes, or post-remagnetization tilt, or a drastically different age of component B.

5. Interpretation and discussion

Following usual procedures, reference declinations and paleolatitudes are calculated from apparent polar wander paths, APWPs, of major cratonic blocks, and we used the APWPs of Baltica and Siberia to compute these parameters for a common point at 41.8°N, 73.8°E. The reference paleolatitude plots for Baltica and Siberia (Fig. 14) are very similar for the NTZ in the 200–360 Ma interval, diverge slightly in the Devonian, and converge again by the Devonian–Silurian boundary. Recent studies (Kravchinsky et al., 2002) of Upper Devonian–Lower Carboniferous volcanics from Siberia showed that the previously used poles of these ages are less reliable; hence we replaced the Carboniferous–Devonian segment of the Siberian paleolatitude plot by a paleolatitude recalculated from this new pole (Kravchinsky et al., 2002). We are aware of a Silurian paleomagnetic result from the Tuva mobile belt (Bachtadse et al., 1999), but have not included it in Siberia's reference curve, because of its significant rotation relative to the craton. In general, Baltica and Siberia middle and late Paleozoic paleolatitudes are too similar for the NTZ for any conclusive test. The predicted latitudes from the Baltica and Siberia reference curves are really different only in the early Paleozoic.

Another source of "reference" data are the reconstructions of tectonic elements within the Ural–Mongol belt suggested by different researchers. The most detailed sets of reconstructions were proposed by Sengör and Natal'in (1996) and Didenko et al. (1994). We read the paleolatitudes (SN and D data, respectively) from their palinspastic maps allowing for $\pm 5°$ error of each reading. Though the NTZ in Sengör and Natal'in's reconstruction is not rigidly attached to Baltica during the early–middle Paleozoic, relative motion between them was smaller than their common latitudinal shift, which is derived from the Baltic APWP. Hence it is not surprising that the Baltic and SN reference paleolatitudes are in very good agreement (Fig. 14). In contrast, a slower and monotonous shift of the NTZ at low northern latitudes is predicted by Didenko et al. (1994).

The polarity of Permian overprint directions and the Carboniferous directions of the Dungurma Fm. is definitely known as reversed, and the observed paleolatitudes closely fit the reference data (Table 9; Fig. 14). Observed paleolatitudes of Ordovician rocks fall in a narrow interval and are statistically indistinguishable (Table 9), but the polarity of the Ordovician HTCs is not a priori known (see the two polarity options in Fig. 14). Despite the considerable scatter, the Ordovician HTC directions are generally aligned N–S; similar alignment is observed for the Carboniferous and Permian directions. If the Ordovician vectors with northerly declinations and shallow negative inclinations correspond to normal polarity, the NTZ was at low southern paleolatitudes and moved subsequently northward without large changes in its orientation with respect to the meridional grid. According to this scenario, the NTZ moved from 9°S to 16°N with average poleward velocity of ca. 2 cm/year between the Caradocian and the Bashkirian, i.e. during about 130 My or less (Fig. 14). The opposite choice of polarity puts the North Tien Shan at low northern latitudes (Fig. 14) but its orientation is then reversed ("upside down"). With this option, the area moved northward by just about 7°, but rotated through about 180° during the same 130 My interval or shorter.

A unique polarity choice could be made if reliable Devonian–Silurian paleomagnetic data from the NTZ

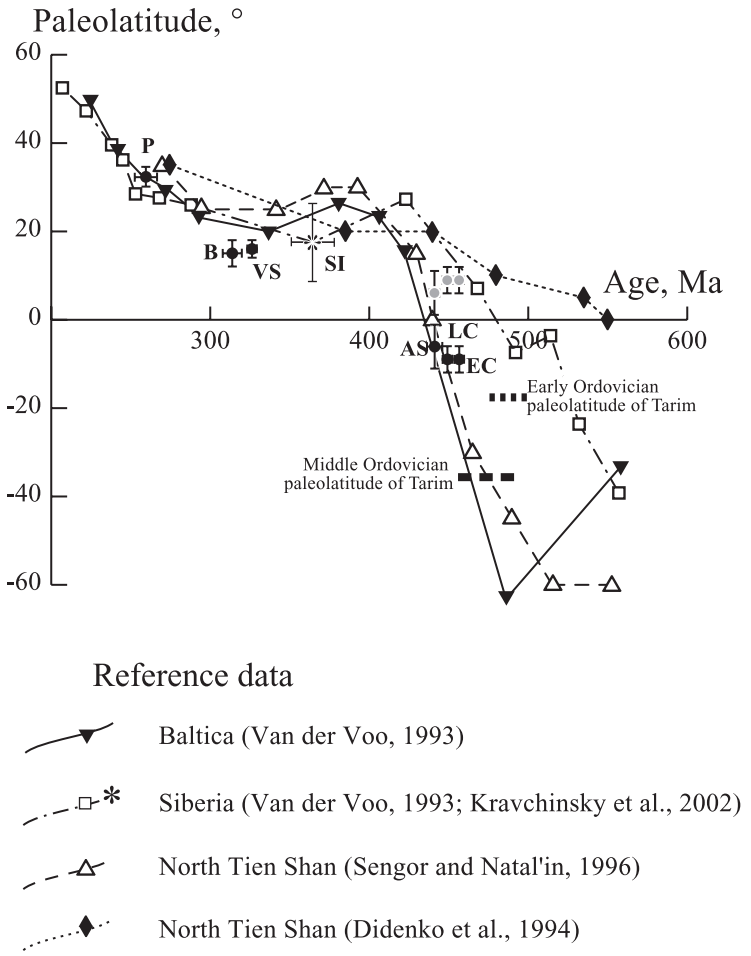

Fig. 14. Plots of paleolatitude versus age for measured (dots) and reference (square, diamond, asterisk, and triangles) data for the North Tien Shan (reference point at 41.8°N, 73.8°E). Upright triangles and diamonds are the reference curves for the North Tien Shan taken from palinspastic reconstructions by Sengör and Natal'in (1996) and Didenko et al. (1994), respectively. The other two reference curves are calculated from the APWPs of Baltica (solid inverted triangles) and Siberia (open squares) from Van der Voo (1993); the poorly defined middle Paleozoic segment of the Siberian reference curve is replaced by a Late Devonian–Early Carboniferous paleolatitude (asterisk, SI) calculated with its confidence limits from a new pole for Siberia (Kravchinsky et al., 2002). Solid dots with vertical and horizontal bars are measured paleolatitudes with confidence limits; also shown are the measured Ordovician latitudes (dot with shaded fill) for the opposite polarity option (see text for detail). P, overall mean of Permian overprints; B, VS, AS, LC, and EC, HTCs in Bashkirian, Visean–Serpukhovian (Dungurma Fm.), Ashgillian, Upper Caradocian (Toluk and Tabylgaty areas combined), and Lower Caradocian rocks (Almaly Fm.), respectively. Ages assigned to the results are from Table 9. Also shown as thick dashed and dotted lines are the Middle Ordovician paleolatitude of 36.5°S (Zhao et al., 1997) and the Early Ordovician paleolatitude of 18.6°S (Fang et al., 1996) for North Tarim.

were available. Middle–Late Devonian (Burtman et al., 1998) and Early Devonian (Klishevich and Khramov, 1993) paleomagnetic directions from the North Tien Shan are generally aligned N–S, with the vectors of normal polarity pointing to the north. Thus a rotation of the NTZ, if any, had to be nearly over by the Early Devonian. These data, however, are based on components and remagnetization circles identified mostly at intermediate temperatures, and their reliability needs to be ascertained.

There is no direct correspondence between angular velocity of a plate and declination change, these parameters being connected in a complex manner (Perroud, 1982). A rotation through 180°, however,

Table 9
Summary table of paleomagnetic results from the North Tien Shan

Result	Age, Ma	Directions				Plat	Poles		
		D (°)	I (°)	k	α_{95} (°)		F (°)	L (°)	α_{95} (°)
P	260 ± 7	–	49.7	51	2.6	30.5 ± 2°N	*73.6*	*200.8*	*4.2*
B	314 ± 6	27.6	28.3	100	5.2	15 ± 3°N	53.8	202.1	4.2
VS	326 ± 3	344.1	31.2	39	6.4	16 ± 2°N	61.6	287.2	5.4
AS	443 ± 5	336.6	– 11.1	48	8.8	6 ± 5°S	37.4	281.1	6.3
LC	450 ± 3	–	– 16.7	48	5.0	9 ± 3°S	*38.2*	*246.5*	*9.0*
EC	456 ± 3	31.1	– 17.7	110	4.0	9 ± 3°S	31.1	214.7	2.9

Results: P, overall mean of Permian overprints in Carboniferous redbeds and Upper Caradocian rocks from the Toluk area; B, VS, AS, LC, and EC, HTC in Bashkirian, Visean–Serpukhovian (Dungurma Fm.), Ashgillian, Upper Caradocian (Toluk and Tabylgaty areas combined), and Lower Caradocian rocks, respectively. Ages are assigned according to the DNAG time scale (after Palmer, 1983). All data are presented as normal polarity directions; paleopoles are given by F = latitude and L = longitude. For strongly elongated data sets (P, LC,), mean inclinations and statistical parameters were calculated after McFadden and Reid (1982), in order to present the best estimate of the area's paleolatitude (Plat). Overall means for the same data sets were also calculated using Fisher (1953), and were used to compute pole positions (in italics); these poles would give paleolatitudes slightly different from those listed as calculated from inclination-only data.

is a special case, and these parameters then correspond to each other provided that a plate remains at low latitudes. Hence the angular velocity of the NTZ had to be ca. 1.5°/My, if the rotation occupied the entire 130 Ma interval, and was more than 4°/My if the rotation terminated by the end of the Silurian, as indicated by the Devonian data. The first value, let alone the second one, is much higher than known angular velocities of the major plates, even rapidly moving purely oceanic ones, for the last 165 My (Engebretson et al., 1985). In general, any rapid rotation of a continent-size block through 180° without a noticeable latitudinal shift is difficult to fit into the framework of plate tectonics. All in all, we cannot definitely exclude the reversed polarity option, but it seems unlikely; hence the discussion below assumes the normal polarity of northward-pointing Ordovician directions.

Early, Late Caradocian and Ashgillian paleolatitudes are similar to a degree, which may be accounted for in several ways. It may indicate the absence of latitudinal displacement, which does not seem to be likely in view of very fast northward motion of Baltica and attached (?) North Tien Shan in the Ordovician. Another explanation takes into account the fact that the age of redbed remanences is constrained no better than predating the latest Ordovician (i.e. Ashgillian)–Early Silurian deformation in this region; hence it may be possible that all redbeds were actually remagnetized in the Ashgillian but before folding; the presence of both polarities, however, is a (weak) argument against this. It may also be that the presumed differences in rock ages are much smaller. The true ages of Lower and Upper Caradocian rocks may be similar indeed; in the West Kyrgyz Range, however, the geological relationship between Lower Caradocian and Ashgillian redbeds precludes the possibility of these rocks having similar ages. Finally, the early Paleozoic poles of Baltica are scarce (Van der Voo, 1993); therefore, the reference paleolatitudes may be in error too. In view of all these ambiguities, we abstain from quantitative estimates and just point to general agreement of measured and reference values.

The good fit between the NTZ and Baltic paleolatitudes (Fig. 14) indicates coherent motion of these two units since the Caradocian, despite the Urals fold belt between them (Fig. 1a). In turn, this good fit rules out the model of Didenko et al. (1994), while it is compatible with the model of Sengör and Natal'in (1996). More early Paleozoic data are needed, however, to confirm the latter model.

Despite considerable distances between the three study areas and rather complex structure of the NTS, Toluk, Tabylgaty, and West Kyrgyz Range, Caradocian mean declinations are generally similar. It indicates that no large-scale relative rotations took place afterwards and that the NTZ already existed as a coherent unit since the Caradocian. On the other hand, the Caradocian and Ashgillian declinations collectively form a girdle distribution, the end-members of which are the Ashgillian and Early Caradocian data from the West Kyrgyz Range; hence the NTZ did not

behave as a rigid body. To the same effect speak the Permian directions, which are also distributed along a small circle (Fig. 13). The Carboniferous data indicate local rotations as well. We conclude that local rotations as young as Late Permian occurred within the NTZ, in accord with geological data and earlier analyses (Bazhenov et al., 1999). Apparently widespread local rotations prevent us from interpreting declination data on anything but a very broad scale. Another reason is that all models of the Ural–Mongol belt (Didenko et al., 1994; Dobretsov et al., 1995; Sengör and Natal'in, 1996) predict rather complicated deformation and rotation of tectonic units, and a stringent test cannot yet be performed with the available declination data.

So far, we compared the kinematics of the NTZ with those of Baltica and Siberia. The third major block bounding the Ural–Mongol belt is Tarim in the south (Fig. 1). The Turkestan ocean is known to have existed between the North and Central Tien Shan on one side and the Tarim block on the other in the middle Paleozoic, probably in early Paleozoic too, and its closure in the Middle Carboniferous resulted in the formation of the late Paleozoic (Variscan) South Tien Shan fold belt (Fig. 1b) (Biske et al., 1985; Biske, 1995). There are two Early to Middle Ordovician paleomagnetic results from Tarim (Fang et al., 1996; Zhao et al., 1997), which place this block at 18.6°S and 36.5°S (see Fig. 14), whereas our Late (!) Ordovician paleolatitude of the North Tien Shan is about 9°S. Unfortunately, the uncertainties in these somewhat preliminary results from Tarim and the difference in the ages of our studies and those for Tarim preclude a reliable conclusion on the width of the Turkestan Ocean. New paleomagnetic data on different intervals of the early Paleozoic are needed both from the Tien Shan and Tarim to clarify the situation.

Acknowledgements

We thank Nina Dvorova for paleomagnetic measurements and Baochun Huang and Boris Natal'in for constructive reviews. This study was supported by the Division of Earth Sciences, the U.S. National Science Foundation, grant EAR 99-09231, grants 00-05-64149 and 00-05-64646 from the Russian Foundation of Basic Research, and grant 7KSPJ065518 (to AVM) from the Swiss National Science Foundation (SNSF).

References

Alexeiev, D.V., Cook, H.E., Mikolaichuk, A.V., Dzenchuraeva, A.V., 2000. New data on the evolution of passive margin carbonate platforms of the Kazakhstania Paleocontinent (abstract). Permo-Carboniferous Carbonate Platforms and Reefs. Society for Sedimentary Geology, El Paso, TX, May 15–16, 2000, 19.

Audibert, M., Bazhenov, M.L., 1992. Permian paleomagnetism of the North Tien Shan: tectonic implications. Tectonics 11, 1057–1070.

Avdeev, A.V., Kovalev, A.S., 1989. Ophiolites and Evolution of the Southwest Part of the Ural–Mongol Fold Belt. Moscow State University, Moscow. 227 pp. (in Russian).

Bachtadse, V., Pavlov, V.E., Kazansky, A.Y., Tait, J., 1999. Paleomagnetism of the Tuva Terrane (Southern Siberia, Russia): implications for the paleogeography of Siberia. J. Geophys. Res. 105, 13509–13518.

Bazhenov, M.L., Burtman, V.S., Dvorova, A.V., 1999. Permian paleomagnetism of the Tien Shan fold belt, Central Asia: the succession and style of tectonic deformation. Tectonophysics 312, 303–329.

Biske, G.S., 1995. Late Paleozoic collision of the Tarim and Kyrgyz–Kazakhstan paleocontinents. Geotectonics 29 (1), 31–39 (in Russian).

Biske, G.S., Zubtsov, E.I., Porshnyakov, G.S., 1985. The Hercynides of the Atbashi–Kokshaal part of the South Tien Shan. LGU, Leningrad. 192 pp. (in Russian).

Burtman, V.S., 1999. Some problems of the Paleozoic tectonic reconstructions in Central Asia. Geotectonics 31 (3), 103–112.

Burtman, V.S., Gurary, G.Z., Belenky, A.V., Ignatiev, A.V., Audibert, M., 1998. The Turkestan ocean in the middle Paleozoic: a reconstruction based on paleomagnetic data from the Tien Shan. Geotectonics 30 (1), 15–26.

Degtyarev, K.E., Mikolaichuk, A.V., 1998. Early Ordovician collisional zone of the North Tien Shan and South Kazakhstan. Proceedings of "Tectonics and Geodynamics: General and Regional Problems". GEOS, Moscow, pp. 160–162. (in Russian).

Didenko, A.L., Morozov, O.L., 1999. Geology and paleomagnetism of middle–upper Paleozoic rocks from the Saur Range. Geotectonics 31 (4), 64–80.

Didenko, A.L., Mossakovsky, A.A., Pechersky, D.M., Ruzhentsev, S.V., Samygin, S.G., Kheraskova, T.N., 1994. Geodynamics of paleozoic oceans of central Asia. Geol. Geofiz. 35 (7–8), 118–145 (in Russian).

Dobretsov, N.L., Berzin, N.A., Buslov, M.M., 1995. Opening and tectonic evolution of the Paleoasian ocean. Int. Geol. Rev. 37, 335–360.

Engebretson, D.C., Cox, A., Gordon, R.G., 1985. Relative motions between oceanic and continental plates in the pacific basin. Bull. Geol. Soc. Am., Spec. Pap. 206, 1–59.

Fang, D.J., Jin, G.H., Jiang, L.P., Wang, P.Y., Wang, Z.L., 1996.

Paleozoic paleomagnetic results and the tectonic significance of Tarim Plate. Chin. J. Geophys. 39 (4), 522–532 (in Chinese).
Fisher, R.A., 1953. Dispersion on a sphere. Proc. R. Soc. London, Ser. A 217, 295–305.
Galitskaya, A.Y., Korolev, V.G., 1961. The Carboniferous of North Kyrgyzia. Reports on Geology of the Tien Shan, issue 1, Akad. Nauk KyrgSSR, 43–75 (in Russian).
Grishin, D.V., Pechersky, D.M., Degtyarev, K.E., 1997. Paleomagnetism and reconstruction of middle Paleozoic structure of Central Kazakhstan. Geotectonics 31 (1), 71–81.
Kirschvink, J.L., 1980. The least-square line and plane and the analysis of palaeomagnetic data. Geophys. J. R. Astron. Soc. 62, 699–718.
Kiselev, V.V., 1999. The U–Pb (by zircons) geochronology of magmatic suits of the Northern Tien Shan. Proceed. National Acad. Sci. of Kyrghyz Republic, Bishkek, Problems of Geology and Geography in Kyrgyzstan, pp. 21–33. (in Russian).
Klishevich, V.L., Khramov, A.N., 1993. Reconstruction of the Turkestan ocean (South Tien-Shan) in the early devonian. Geotectonics 27 (4), 66–75 (in Russian).
Kravchinsky, V.A., Konstantinov, K.M., Courtillot, V., Savrasov, J.I., Valet, J.-P., Cherniy, S.D., Mishenin, S.G., Parasotka, B.S., 2002. Palaeomagnetism of East Siberian traps and kimberlites: two new poles and palaeogeographic reconstructions at about 360 and 250Ma. Geophys. J. Int. 148, 1–33.
Lomize, M.G., Demina, L.I., Zarshchicov, A.V., 1997. The Kyrgyz–Terskey paleoceanic basin in the Tien Shan. Geotectonics 31 (6), 463–482.
Mazarovich, O.A., Barskov, I.S., Borisenok, V.I., Lomize, M.G., Sobolev, R.N., Filatova, L.I., 1995. Northern Sinjiang in system of Central Asia Paleozoids. MOIP Bull. 10 (6), 3–21 (in Russian).
McFadden, P.L., Jones, D.L., 1981. The fold test in palaeomagnetism. Geophys. J. R. Astron. Soc. 67, 53–58.
McFadden, P.L., McElhinny, M.W., 1988. The combined analysis of remagnetization circles and direct observations in palaeomagnetism. Earth Planet. Sci. Lett. 87, 161–172.
McFadden, P.L., Reid, A.B., 1982. Analysis of paleomagnetic inclination data. Geophys. J. R. Astron. Soc. 69, 307–319.
Mikolaichuk, A.V., Kotov, V.V., Kuzikov, S.I., 1995. The structural position of the Malyi Naryn metamorphic complex and the boundary between the North and Middle Tien Shan. Geotectonics 29 (2), 157–166.
Mikolaichuk, A.V., Kurenkov, S.A., Degtyarev, K.E., Rubtsov, V.I., 1997. Main stages of geodynamic evolution of the North Tien Shan in the late Precambrian and early Paleozoic. Geotectonics 31 (6), 16–34.
Misius, P.P., 1986. Ordovician Brachiopods of North Kyrgyzia. Ilim. Frunze. 180 pp. (in Russian).
Misius, P.P., 1993. New data on the Ordovician Toluk Suite of the North Tien Shan. In: Bakirov, A.B. (Ed.). New Biostratigraphic Results on the Precambrian and Paleozoic of Kyrgyzstan. Ilim, Bishkek, pp. 81–92. (in Russian).
Mossakovsky, A.A., Ruzhentsev, S.V., Samygin, S.G., Kheraskova, T.N., 1993. Geodynamic evolution of the Central-Asia folded belt and history of its development. Geotectonics 27 (6), 3–32.
Nikitin, I.F., 1972. The Ordovician of Kazakhstan: Vol. 1. Stratigraphy. Nauka, Alma-Ata. 242 pp. (in Russian).
Nikitin, I.F., 1973. The Ordovician of Kazakhstan: Vol. 2. Paleogeography, Paleotectonics. Nauka, Alma-Ata. 110 pp. (in Russian).
Opdyke, N.D., Channell, J.E.T., 1996. Magnetic stratigraphy. Intern. Geophys. Series, vol. 64. Academic Press, London, p. 346.
Opdyke, N.D., Roberts, J., Claoue-Long, J., Irving, E., Jones, P.J., 2000. Base of the Kiaman: its definition and global stratigraphic significance. Geol. Soc. Amer. Bull. 112, 1315–1341.
Palmer, A.R., 1983. The decade of North American geology (DNAG) 1983 geologic time scale. Geology 11, 503–504.
Pechersky, D.M., Didenko, A.N., 1995. The Paleoasian Ocean. OIFZ, Moscow. 296 pp. (in Russian).
Perroud, H., 1982. Change of palaeomagnetic vector orientations induced by Eulerian rotations: applications for the relative rotations of Spain and Europe. Tectonophysics 81, 15–23.
Sengör, A.M.C., Natal'in, B.A., 1996. Paleotectonics of Asia: fragments of a synthesis. In: Yin, A., Harrison, M. (Eds.). The Tectonic Evolution of Asia. Cambridge Univ. Press, Cambridge, pp. 486–640.
Sengör, A.M.C., Natal'in, B.A., Burtman, V.S., 1993. Evolution of the Altaid tectonic collage and Palaeozoic crustal growth in Eurasia. Nature 364, 299–307.
Torsvik, T.H., Trench, A., Lohmann, K., Dunn, S., 1995. Lower Ordovician reversal asymmetry: an artifact of remagnetization or non dipole field disturbances. J. Geophys. Res. 100, 17885–17898.
Van der Voo, R., 1993. Paleomagnetism of the Atlantic, Tethys and Iapetus Oceans. Cambridge Univ. Press, Cambridge. 411 pp.
Yakubchuk, A.S., 1990. Tectonic position of ophiolite zones in the Paleozoic structure of Central Kazakhstan. Geotectonics 5, 55–68 (in Russian).
Zamaletdinov, T.S., Osmonbetov, K.O., 1988. Geodynamic model of the Kirgizia Earth crust evolution during the Phanerozoic. Sov. Geol. 1, 66–75 (in Russian).
Zhao, X., Coe, R.S., Smith, R.M., Wu, H., Xie, D.K., Gilder, S.A., Pfoutz, H., 1997. New Cambrian and Ordovician paleomagnetic poles from Tarim and their paleogeographic implications. EOS Trans. AGU, Fall Meet. Suppl. 78, F175.
Zijderveld, J.D.A., 1967. AC demagnetization of rocks: analysis of results. In: Collinson, D.W., Creer, K.M. (Eds.). Methods in Paleomagnetism. Elsevier, Amsterdam, pp. 254–286.
Zima, M.B., Maksumova, R.A., 1990. The Ordovician of the Kara–Jorgo Range (North Tien Shan). Izv. Akad. Nauk SSSR, Ser. Geol. 2, 74–81 (in Russian).